UNIVERSIDAD NACIONAL DE COLOMBIA

Influence of atlas-based and patient dependent forward models in EEG source reconstruction

Influencia de modelos directos paciente-dependientes y basados en atlas en la reconstrucción de fuentes con EEG

Yohan Ricardo Céspedes Villar

Universidad Nacional de Colombia
Faculty of Engineering and Architecture
Department of Electrical, Electronic and Computer Engineering
Manizales, Colombia
2017

Influence of atlas-based and patient dependent forward models in EEG source reconstruction

Influencia de modelos directos paciente-dependientes y basados en atlas en la reconstrucción de fuentes de EEG

Yohan Ricardo Céspedes Villar

Thesis presented as partial requirement to obtain the degree:
Master of Engineering

Advisor:
Ph.D. Germán Castellanos Domínguez
co-Advisor:
Ph.D. Juan David Martínez Vargas

Research Area:
Digital Signal Processing
Research Group:
Signal Processing and Recognition Group

Universidad Nacional de Colombia
Faculty of Engineering and Architecture
Department of Electrical, Electronic and Computer Engineering
Manizales, Colombia
2017

Acknowledgements

It is impossible to name each one of the people who in one way or another have helped me get here. My sincere apologies in advance to those whom I forget to mention.

I am especially grateful to my adviser Germán Castellanos Domínguez and co-advisor Juan David Martínez Vargas for always providing their knowledge, experience, guidance, patience and dedication to this thesis. Also, I would like to thank Ernesto Cuartas Morales, who helped me understand and discuss several findings of this work.

Likewise, I express my gratitude to all members of the Signal Processing and Recognition Group for their support and enrichment of my academic and personal life.

Finally, I want to dedicate this work to my parents, Elizabeth y Alfonso, they made it possible!!!

Yohan Céspedes

This research was carried out under the project: *Desarrollo de un sistema de soporte diagnóstico y detección temprana de Alzheimer basado en medidas de conectividad funcional a partir de registros electroencefalográficos en estado de reposo* - Código: 111974455497.

Abstract

Electroencephalography Source Imaging (ESI) techniques have become the most attractive alternative to support the estimation of neuronal activity through the mapping of electrical potentials measured over the scalp. It takes advantage of the low implementation cost, the high temporal resolution, and non-invasiveness in the patient. ESI techniques require a volumetric conductor model (commonly named Electroencephalography (EEG) Forward Model), including information about the physiological and geometrical properties of the head, and modeling the electromagnetic field propagation of the neuronal activity throughout the head tissues to reach the scalp. In this regard, the accuracy of ESI solutions depends partially on the capabilities of the forward model to correctly describe the structural information provided by a Magnetic Resonance Image (MRI). However, acquiring MRIs for generating personalized head models is expensive, slow, and in some cases unpractical. In this work, we investigate how the head model influences the source reconstruction based on EEG when progressively including different levels of prior structural information. Hence, we evaluate two approaches to enhance the model of brain structure in the EEG forward problem formulation. First, the incorporation of different brain tissue morphology, mainly, based on a Generic MRI, based on a target population Atlas, or based on a patient-specific MRI. Second, the variation of the tissue model complexity in the number of segmented brain layers. All the head models are build using the Finite Difference Reciprocity Method (FDRM). Model comparison is carried out under a Parametric Empirical Bayesian (PEB) framework using Event-Related Potentials (ERPs) taken from the studied population. Obtained results show that the more realistic and subject dependent model, the better performance of the ESI solution.

Keywords: EEG, Forward model, ESI, BMS.

Resumen

Las técnicas de reconstrucción de fuentes basadas en Electroencefalografía (ESI) son la alternativa más interesante para la estimación de fuentes mediante los potenciales eléctricos medidos sobre el cuero cabelludo, aprovechando el bajo costo de implementación, la alta resolución temporal, y la poca invasión que requiere en el paciente. Es por esto, que estas técnicas requieren un modelo de conducción volumétrico (comúnmente llamado modelo directo), que incluye información de las propiedades físicas y geométricas de la cabeza, ademÃ¡s de modelar la propagación del campo electromagnético generado por la actividad neuronal a través de los diferentes tejidos de la cabeza hasta alcanzar el cuero cabelludo. En este sentido, el correcto desempeño de las técnicas ESI depende directamente de las capacidades del modelo directo para describir de manera apropiada la información estructural aportada por una Imagen por Resonancia Magnética (MRI). Sin embargo, adquirir MRIs para generar modelos de la cabeza personalizados, es costoso, lento, y en algunos casos poco práctico. En este trabajo, se investiga la manera en que el modelo directo influencia la tarea de reconstrucción de fuentes basada en EEG, incluyendo de manera progresiva diferentes niveles de información estructural relacionada al paciente. Así, se evaluan dos enfoques específicos para mejorar el modelo de la estructura cerebral en la formulación del problema directo de EEG. El primer enfoque está relacionado con la incorporación de diferentes morfologías de tejido cerebral, principalmente, basadas en un MRI genérico, un atlas de la población estudiada, ó en el MRI específico del paciente. El segundo enfoque es la variación de la complejidad del modelo en términos de el número de tejidos segmentados en el cerebro. En este trabajo el modelo directo se soluciona usando el Método de Diferencias Finitas con Reciprocidad (FDRM). La comparación de modelos se realiza bajo un *framework* Bayesiano Empírico Paramétrico (PEB), que permite contrastar los diferentes enfoques del modelo directo, usando datos reales. En general, los resultados obtenidos muestran que usar modelos más realistas y más dependientes de la población de estudio, mejora significativamente el desempeño de las técnicas ESI.

Palabras clave: EEG, Modelo directo, ESI, BMS.

List of Figures

Contents

1 Preliminaries

1.1. Introduction

The neuroscience arises from the brain study, making the complete understanding of brain functioning of great interest in applications as treatment of some brain diseases or interpretation of the human cognitive processes. However, one of the most limiting problems is the detection and extraction of functional information related to the brain. Hence, non-invasive techniques have been developed to extract information about brain functions, based on the measurement of electrophysiological, hemodynamic, metabolic and neurochemical processes caused by the functioning of the human brain [3]. Most representative methods include Positron Emission Tomography (PET), functional Magnetic Resonance Imaging (fMRI), functional Near-Infrared Spectroscopy (fNIRS), among others. These techniques offer an excellent spatial resolution, favoring the precise identification of active areas related to particular brain states [60]. Nonetheless, such methods are expensive and, mostly, offer a poor temporal resolution, reducing the possibility of analyzing temporal dynamics in the brain.

Additionally, other methods can also be used to study the brain functioning, among them, Magnetoencephalography (MEG) and Electroencephalography (EEG) [27]. These techniques offer a high temporal resolution, allowing the characterization of brain activity with milliseconds time resolution [41]. EEG is most used than MEG and the methods mentioned above, primarily because of the lower implementation cost. For this reason, the EEG signals are widely used in applications that require a better temporal resolution for monitoring the brain dynamics. Nevertheless, EEG recordings indirectly provide spatial information due to they are measured by electrodes disposed on the scalp. Thus, when EEG data are combined with structural information, as the provided by the Magnetic Resonance Images (MRI), it opens the possibility of determining the location of activity sources in the brain. This process is referred to as EEG source imaging (ESI).

ESI Solutions in general needs two different components working together. First, a volumetric conductivity model (commonly known as EEG forward model or head model) including information about the physical and geometrical properties of the head for describing the electromagnetic field propagation of the neuronal activity throughout the head tissues to reach the scalp [58]. Second, a source localization technique (also known as the inverse solution), that takes advantage of the information provided by the forward model and estimates the possible current sources within the brain associated with the sensor measurements. Thus,

the acquired EEG recordings and the defined head model are used to reconstruct the sources of neuronal activity [19]. Regarding this, estimation of the current sources in the brain is an ill-posed problem, i.e., small variations in the measured data lead to significant changes in the result, generating non-uniqueness of solutions. This unstable behavior is due to the number of electrodes measuring the electrical activity is relatively small respect to the discretized brain activity sources, additionally to the lousy signal to noise ratio in the EEG. To deal with this effect of non-uniqueness is necessary to include more information about the head structure and the temporal dynamics to constraint the result to a unique and optimal solution [19]. Thus, the head model generation should be influenced by information reflecting anatomical and physical properties of the head compartments (the named prior information). Consequently, the accuracy of ESI solutions depends partially on the capabilities of the forward model to correctly describe the structural information provided by an MRI or a Computerized Tomography (CT). Nevertheless, acquiring MRIs for generating personalized head models is expensive, and in some cases unpractical. In consequence, a template MRI is used when patient-specific anatomical images are not available. As a result, head models are commonly constructed based on the anatomy of an arbitrary subject not belonging to the patient or population under study (template head models) [63]. However, diverse works have shown that source localization is enhanced in ESI when the physical properties of the head are modeled with the information provided by the patient-specific MRI [22, 56, 10].

Regarding the Forward Model computation, an analytical solution is only possible for particular cases whit a highly symmetrical head geometry. For more general cases, numerical methods are required, allowing to solve volume conductor head models with free form and enabling the estimation of the electrical potentials at any location in the volume. There are several numerical methods to obtain a forward solution, among them spherical models, Boundary Finite Elements (BEM), Finite Elements Method (FEM), Finite Difference Method (FDM), Finite Difference Reciprocity Method (FDRM) and Finite Volume Method (FVM) [9, 42, 20, 16]. For a basic head modeling, a 3-Layers template head volume made with boundary element method (BEM) is often used, including scalp, skull and brain compartments [58]. However, these models usually do not include cerebrospinal fluid (CSF) and white matter (WM), which affect the current-flow between sources and electrodes. Besides, BEM solves the forward potentials only for the interfaces between two neighbor tissues. As a result, BEM interpolates the potential in the scalp induced by a dipole inside the GM. In this work, we used FDRM since MRI data is usually acquired in regular formats of digitalization, that can be adapted to a regular grid.

This work is focused on one of the principal topics on ESI, specifically, the forward model of the EEG data. We investigate how the head model influences the source reconstruction based on EEG when we progressively include different levels of prior structural information. In this regard, we evaluate two approaches to enhance the model of brain structure in the EEG forward problem formulation. First, the progressive incorporation of the brain tissue morphology, mainly, based on a Generic MRI, based on a target population Atlas, or based on

a patient-specific MRI. Second, the variation of the tissue model complexity by augmenting the number of segmented brain layers. The mixing of the aforementioned levels of model complexity and the different anatomic structure priors give a set of nine testing scenarios. The scenarios comparison is made regarding the achieved ESI precision. We use a Bayesian approach to invert the forward model. Concretely, we use Multiple Sparse Priors (MSP) and Low-Resolution Tomography (LOR) techniques, which provide an alternative for testing forward models using real data. The measuring of performance is made with the model evidence corresponding to each scenario. We evaluated the testing scenarios using real-world data of 25 subjects. Obtained results prove that more accurate and realistic forward models will lead to more precise ESI solutions.

1.2. Objectives

Based on the previously mentioned open issues, we develop this work around one general objective, which is divided into three specific objectives, as follows:

1.2.1. General Objective

To develop a methodology for generating realistic and personalized conductivity head models, that includes the geometry of different brain structures (gray matter, white matter, CSF, skull, scalp). Head models should improve the performance of Electroencephalographic Source Imaging on Event Related Potentials (ERPs) data.

1.2.2. Specific Objectives

1. To propose a methodology for generating personalized forward models, allowing the inclusion of prior structural information and different levels of model complexity.

2. To develop a methodology for estimating a neural source space using patient-specific structural information.

3. To evaluate and compare the performance of forward models in the EEG source reconstruction task.

1.3. Outline

The present research work is divided into three more chapters and can be read as follows:

In chapter 2 a review of the main topics behind the ESI techniques are given to put in perspective the focus of this work. In the first section, considering that the neuroimaging

arises from the brain study, we briefly describe the anatomy and physiology of the brain. In the second part, we introduce the EEG concept and summarize the recording process and relevant applications. The third section is fixed to describe the principles of EEG forward modeling. Thus, we establish the current dipole as source simplification and define the reason why is necessary a representation of the electromagnetic and geometrical properties of the head, modeling the field propagation of the current dipoles to the electrodes. Hence, we introduce the algebraic representation of the forward model and provide the numerical framework employed for the solution. A pipeline description of the proposed methodology for head model estimation is provided at the end. The final section is destined to present the Bayesian Framework to solve the inverse problem in the ESI task, as well as define tools for the measure, evaluation and comparison of the head models performance. We start by describing the Bayes' theorem and follow introducing the Bayesian formulation of the EEG inverse problem. Next, we describe an approach to add multiple priors concerning covariance components, as well as the free energy cost function optimized to obtain a unique solution. By last, we set the free energy as an approximation of the model evidence and explain why it can be employed to compare the performance of different forward models using realistic EEG data.

In the chapter 3 we present a methodology for generating personalized head models, as well as an evaluation of their performance in the reconstruction of neuronal source activity from event-related potentials (ERPs). We evaluate two approaches to enhance the model of brain structure in the EEG forward problem formulation, mainly, the progressive incorporation of closer knowledge of the brain tissue morphology concerning each patient, and the variation of tissue model complexity by augmenting the number of segmented brain layers. Initially, we describe the patient-specific data used in the forward model generation and validation of the proposed methodology. Starting from this, we present a set of testing scenarios, which includes the combination of different levels of model complexity and different prior anatomical structures. The model comparison is made using the Bayesian Model Selection (BMS) framework presented in chapter 2, allowing to evaluate the enhancement of ESI in the different testing scenarios. The last section of this chapter is destined to the discussion of obtained results.
Finally, conclusions and possibilities for future research work are given in chapter 4.

1.4. Academic Discussion

Journal papers
Céspedes-Villar, Y. R., Martínez-Vargas, J. D., Cuartas-Morales, E., & Castellanos-Dominguez, C. (2017, October). Enhanced EEG source imaging using realistic patient-specific head models. *Accepted for revision.*

Indexed conference papers
Céspedes-Villar, Y. R., Cuartas-Morales, E., Martínez-Vargas, J. D., Arteaga-Daza, L. F., & Castellanos-Dominguez, C. (2017, June). Influence of Population Dependent Forward Models on Distributed EEG Source Reconstruction. In International Work-Conference on the Interplay Between Natural and Artificial Computation (pp. 374-383). Springer, Cham.

Conference papers
Céspedes-Villar, Y.R., Arias-Mora, L., López-Ríos, L., Velasquez-Martinez, L. F., Alvarez-Meza, A. M., & Castellanos-Dominguez, G. (2015, September). Kernel-based relevant feature extraction to support Motor Imagery classification. In Signal Processing, Images and Computer Vision (STSIVA), 2015 20th Symposium on (pp. 1-6). IEEE.

Céspedes-Villar, Y.R., Hurtado-Rincon, J., Rojas-Jaramillo, S., Alvarez-Meza, A. M., & Castellanos-Dominguez, G. (2014, September). Motor imagery classification using feature relevance analysis: An emotiv-based bci system. In Image, Signal Processing and Artificial Vision (STSIVA), 2014 XIX Symposium on (pp. 1-5). IEEE.

Software prototypes
Céspedes-Villar, Y.R., Collazos-Huertas, D. F., & Castellanos-Dominguez, G. (2017, August). MultistimulusV2.

Céspedes-Villar, Y.R., Alvarez-Meza, A. M., & Castellanos-Dominguez, G. (2016, April). Relevant feature extraction for motor imagery discrimination - REMI.

2 EEG Source Imaging

2.1. Introduction

Electroencephalographic Source Imaging (ESI) techniques allow the estimation of neuronal activity through the electrical potentials measured over the scalp. EEG is commonly used in the task of source reconstruction because of their advantages in implementation cost, high temporal resolution, and non-invasiveness in the patient. Brain source reconstruction requires three components. First, a recording of the Electroencephalographic (EEG) signals. Second, a correct modeling of the conduction and morphology of the different head compartments. Third, a technique for inverse mapping of the measured activity from electrodes to the sources. In this regard, the accuracy of ESI solutions directly depends on the capabilities of the forward model to properly describe the information provided by individual structural Magnetic Resonance Image (MRI).
This chapter gives a brief review of the aforementioned main topics around the ESI techniques. In the first part, we focus on describing the brain anatomy, beginning with the neuron as a primary component, and generalizing in the description of the brain structures and their functions. In the second part, we summarize the EEG activity recording process, explaining its origin, primary stages, and significant applications. The next section is dedicated to present the head modeling methods employed in this work. Thus, a pipeline description of the methodology for forward model computing is provided. The final section is dedicated to the solution to ESI task under a Bayesian Framework, as well as a method to assess the obtained performance of the estimated head model.

2.2. The brain

The brain is found within the head, covered by several layers of tissues. It is the most complex organ in the human body and serves as the center of the nervous system. Neuroimaging arises from the brain study, being of great importance the knowledge of its basic anatomic components and how they work synergistically. In this sense, to understand the functioning of the brain, it is first necessary to describe its main component, the neuron cell. Briefly, the job of neuron cells consists of receive and transmit information through electric impulses in a complex neuronal network. The communication between two neurons is called synapses [54]. In a human, cerebral cortex contains approximately 100 billion neurons [2, 45, 44, 12, 62,

29, 43, 23], each one connected by synapses to several thousand other neurons. The neurons present typical morphologic features (see Figure **2-1**) [28]:

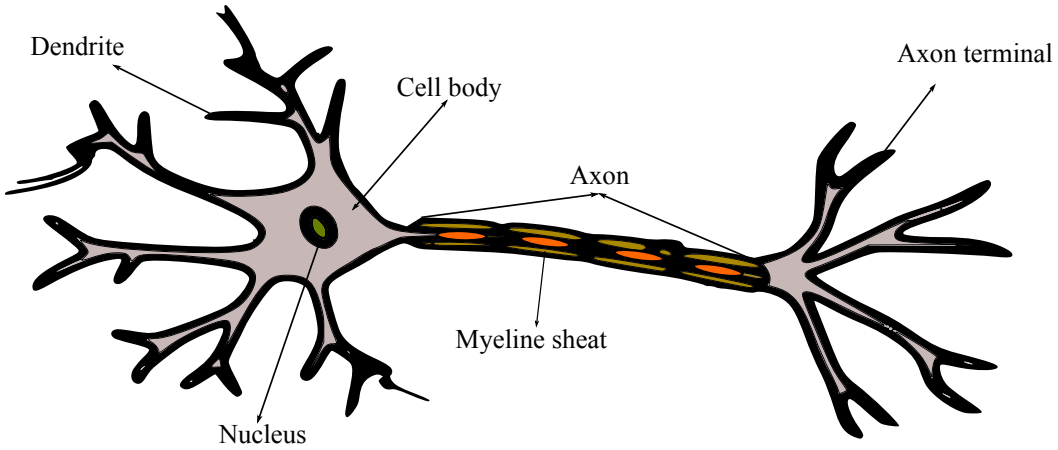

Figure 2-1: neuron Structure: -***Cell body:*** Also named perikaryon or soma. It contends the nucleus and all the components of any eukaryotic cell. -***Nucleus:*** Located at cell body. It contents the information that drives the neuron in his general functioning.-***Dendrites:*** Are prolongations that originate in the cell body. His function is to receive the impulses of others neurons and send it to the cell body.-***Axon:*** It drives the impulses from the cell body towards other neurons. In this section appears the synapses.

Brain structure

As a consequence of biological evolution different anatomical brain structures can be distinguished, mainly characterized by the typical arrangement of their neurons. The oldest part of the brain is known as the brain stem and is responsible for basic vital life functions such as breathing, heartbeat, and blood pressure. Attached to the rear of the brain stem is found the cerebellum, meaning "little brain". It is assumed to be much older than the cerebrum, and its structure is associated with regulation and coordination of movement, posture, and balance. It has two hemispheres and has a highly folded surface. Next, is located the youngest part of the human brain, the cerebrum, which is divided into the left and right hemisphere. The cerebrum or cortex is the largest part of the human brain, associated with higher brain functions such as thought and action. The inner layer of the cerebrum is the white matter, which contains the myelinated axons, also called tracts. The outermost layer of the cerebrum is the cerebral cortex or gray matter, which contain the neurons' cell bodies and dendrites. It is heavily folded resulting in a much greater surface area inside the skull volume. Additionally, the brain is covered by the scalp, skull, cerebrospinal fluid (CSF), among others, which acts as a protective layer for the cerebral cortex. Especially, the CSF serves as a transport conduit for nutrients to the brain and waste from the brain. All these structures can be distinguished in the Figure **2-2**.

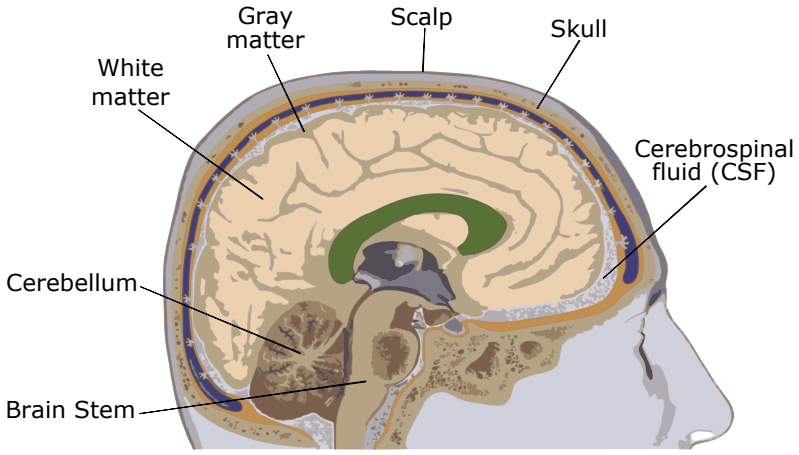

Figure 2-2: Human Head anatomy.

Functional brain regions

The cerebral cortex is divided into four sections, called "lobes": the frontal lobe, parietal lobe, occipital lobe, and temporal lobe. The frontal lobe is associated with reasoning, planning, parts of speech, movement, emotions, and problem-solving. The parietal lobe is associated with movement, orientation, recognition, and stimuli perception. The occipital lobe is related to visual processing. The temporal lobe is associated with perception and recognition of auditory stimuli, memory, and speech. A visual representation of the cortex division is shown in Figure **2-3**. There are different histological structure and organization of neurons, which

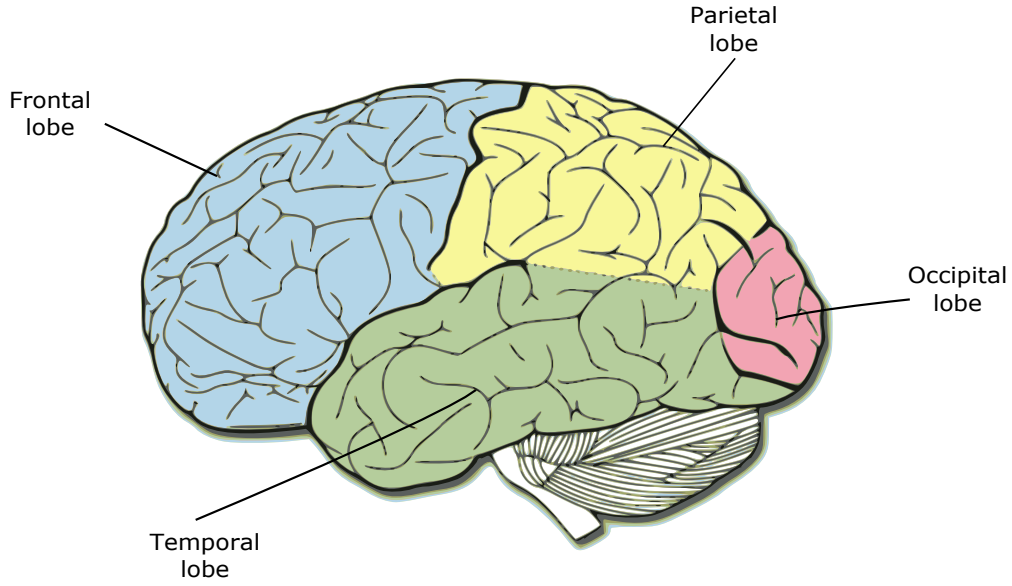

Figure 2-3: Brain division in lobes.

makes each of them special for certain functions. This is how different neocortical regions,

known as the Brodmann areas [17], can be distinguished. Brodmann areas are defined using the neuronal organization and have been correlated closely to diverse cortical functions.

2.3. The Electroencephalography

A set of experiments showing the possibility of measuring and visualizing the electrical activity of the human brain was shown in 1929 by [5]. They were done by the arrangement of electrodes along the scalp, a posterior amplification of the obtained signal, and the graphing over a period. This process was named as Electroencephalography (EEG). Each part of the brain shows a mixture of rhythmic and nonrhythmic activity, which may vary according to behavioral states, making EEG signals ideal for studying brain activity during cognitive processes.
Given that EEG is a relatively cheap and easy applicable technique to record brain activity, it can be applied to various fields: medicine, research, brain-computer interfaces, neuromarketing, among others. For example, EEG is most often used to diagnose epilepsy, which causes abnormalities in EEG readings [59]. It is also used to diagnose sleep disorders, depth of anesthesia, coma, encephalopathies, and brain death. Furthermore, EEG is a first-line method of diagnosis of tumors, stroke and other focal brain disorders [8].

2.3.1. Event Related Potentials (ERPs)

Working with EEG signals is a challenge because they contain the mixed activity of conglomerations from thousands of neuronal sources, making hard the isolation of individual neurocognitive processes. However, it is possible to extract neuronal responses associated with specific sensory, cognitive and motor events embedded within the EEG [37]. These specific responses are known as Event-Related Potentials (ERPs) to denote the fact that there are electrical potentials associated with specific events. The study of the brain in this way provides a noninvasive method for evaluating brain functioning.
The EEG contains thousands of simultaneously ongoing brain processes, i.e., the brain response to an event of interest is not usually visible in the EEG recording of a single trial. To obtain the brain's response to a specific event is necessary to record the EEG for a stimulus several times to average them together, causing random brain activity to be averaged and the response to the specific event to remain.
Ensemble averaging (EA) method has been widely used to extract the ERPs from a noisy background. The method makes two critical assumptions: i) Assumes that on-going background EEG activity is a statistically random process, and will, therefore, be canceled out by averaging over a large number of trials, leaving the non-random ERPs signals. ii) Assumes that ERPs signal is the same or similar for each trial included in the average. An illustrative example of this process is shown in Figure **2-4**. The figure can be read as follows: First, A EEG recording is performed to the subject while a set of stimulus (Target or non-Target)

is presented. Stimuli are marked on the EEG signal, for segmentation purposes. Next, EEG segments are averaged individually for each stimulus. As a result, ERPs are extracted. Figure **2-4** shows the process for the Pz channel but is reproducible for all others.

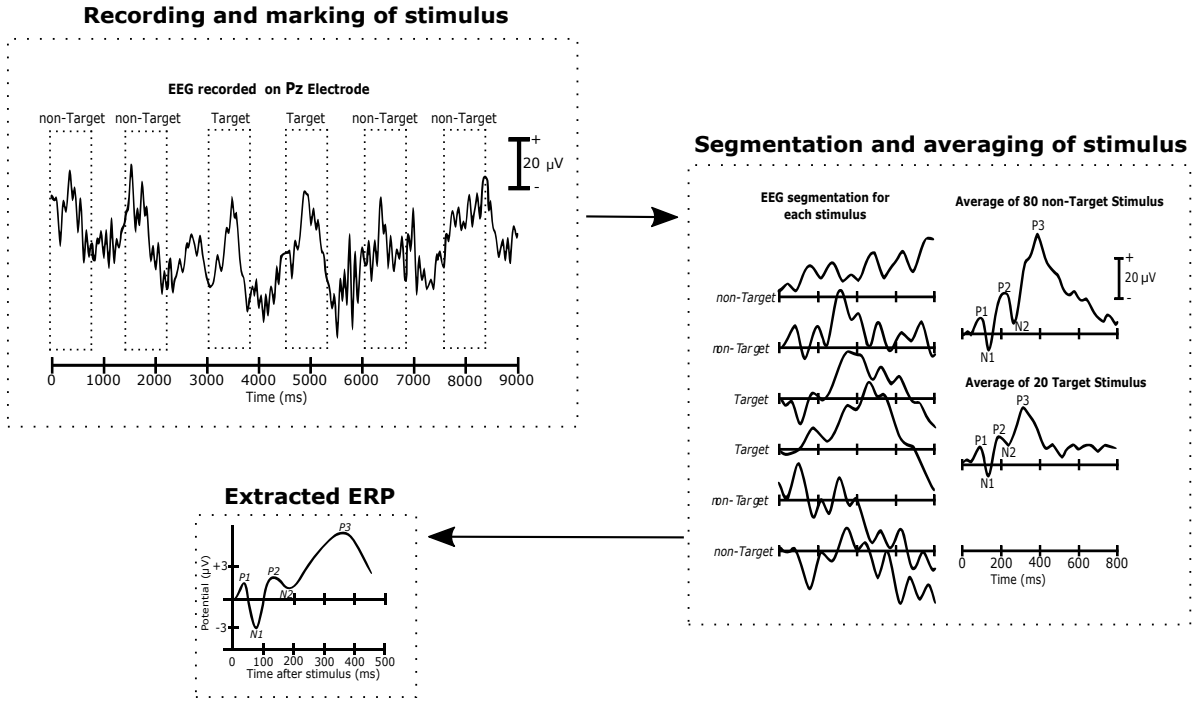

Figure 2-4: Common stages in the extraction of Event Related Potentials

Unfortunately, ERPs signals have variational dynamics across stimulus trials during an experiment. Such variations may be associated with fluctuating attention levels, adoption to stimuli, fatigue, or other unknown factors. Thus EA methods may fail to track trial-to-trial variations both in latency and amplitude. For this reason, different models to extract the relevant information had been employed during past years, including Wiener filter, Adaptive filter, Maximum-Likelihood Method and Autoregressive Process [34, 30, 6, 26, 32].

2.4. EEG Forward Problem

One neuron generates a small amount of electrical activity in the order of Femtoamperes. This small amount cannot be picked up by surface electrodes. When a large group of neurons (approximately 1×10^6 neurons) is simultaneously active, the electrical activity is large enough to be picked up by the electrodes at the surface, thus generating a significant EEG signal [19]. This physical limitation defines the spatial resolution of EEG source imaging. So, the electrical activity of a group of neurons can be modeled as a current dipole. The current flow of the dipole causes an electric field and also a potential field inside the human head, which extends to the scalp. A volume conductor should be constructed to model the

field propagation, by incorporating structural priors about the human head compartments. Commonly, priors are constructed from structural Magnetic Resonance Image (MRI). ESI task requires the volume conductor for modeling the conductivity patterns that allow calculating the propagation of sources towards the electrodes [20]. Modeling the field propagation of sources towards the electrodes generate a projector referred to as the lead field matrix. Thus, the Forward problem consists of calculating the EEG signal when we know the source location.

2.4.1. Mathematical statement of the Forward Problem

In the EEG source imaging (ESI), the EEG forward problem solution involves the estimation of the electrical potentials on the scalp surface Γ_Ω, based on the electrical conductivity and geometry provided by the head volume conductor Ω. Due to the relevant frequencies of the EEG spectrum are below 100 Hz, the quasi-static approximation of Maxwell's equations are used to estimate the potential fields $\boldsymbol{V}(x,y,z) \in \Re$, with $x,y,z \in \Omega$ for a given distribution of N_c electrodes over the scalp ($\boldsymbol{V} \subset \Gamma_\Omega$). Generally, the forward problem solution relies upon the inhomogeneous anisotropic Poisson equation, as follows:

$$\nabla \cdot (\boldsymbol{\Sigma}(x,y,z)\nabla \boldsymbol{V}(x,y,z)) = -\nabla \cdot \boldsymbol{J}(x_{\iota_f}, y_{\iota_f}, z_{\iota_f}), \quad x,y,z \in \Omega \tag{2-1}$$

where $\boldsymbol{J}(x_{\iota_f}, y_{\iota_f}, z_{\iota_f}) \in \Re$ is the electric current density, and values $x_{\iota_f}, y_{\iota_f}, z_{\iota_f} \in \Omega$ represent the position of the current source $\boldsymbol{\iota}_f$, assuming $-\nabla \cdot \boldsymbol{J} = \boldsymbol{\iota}_f$. Moreover, $\boldsymbol{\Sigma}(x,y,z) \in \Re^{3\times 3}$ is the spatially varying inhomogeneous and anisotropy conductivity tensor. In case of the isotropic volumes, the conductivity $\boldsymbol{\Sigma}(x,y,z)$ is scalar-valued, i.e., $\boldsymbol{\Sigma}(x,y,z) = \sigma \boldsymbol{I}$, where $\boldsymbol{I} \in \Re^{3\times 3}$ is the identity matrix, and $\sigma \in \Re^{+}$ is the scalar conductivity value. In this work we only use isotropic conductivities.

2.4.2. Forward Solution

Nonetheless, the solution of Poisson equation for realistic head model depends on requirements that must be carefully fulfilled: i) the boundary conditions between two compartments with different conductivities (Neumann and Dirichlet), and ii) A numerical framework allowing a piecewise solution for the partial differential equations in a volumetric and irregular domain [20, 61]. To this purpose, we solve the potential unknowns only for the original domain Ω, following the particular *Neumman homogeneous* condition in the interface Γ_Ω, where no current can be injected into the air outside the human head. In this regard, Γ_Ω is the boundary limit where the potential values are significant (different to zero). Hence, the original domain Ω holding the interface Γ_Ω fully contains the non-zero forward potentials. Therefore, Equation (2-1) is discretized using the Finite Difference Reciprocity Method (FDRM) formulation [9], building a linear equation for the unknown V_0^j around the stencil

S_j with 18 neighboring vertexes V_i^j for the FDRM solution, as follows:

$$\sum_{i \in S_j}^{18} \alpha_i^j V_i^j - \left(\sum_{i \in S_j}^{18} \alpha_i^j \right) V_0^j = \boldsymbol{\iota}_f, \tag{2-2}$$

where $V_i^j \in \Re$ is the scalar-valued potential at the i-th neighbor vertex of the j-th node in the stencil S_j, $\boldsymbol{\iota}_f \in \Re$ is the dipole current, and $\alpha_i^j \in \Re$ are the FDM coefficients form depending on the conductivity tensor $\boldsymbol{\Sigma}$ and the inter-node distance h [55].
Generally speaking, Equation (2-2) results in a linear system that is solved using *BiCG stabilized* solver with iLU preconditioning [9]. However, the system implementation requires a high computational burden. A pre-calculation of reciprocity potentials is employed to speed up the computation of the inverse solutions. As a result, we calculate a lead field matrix $\boldsymbol{L}_m \in \Re^{N_c \times N_d}$ for a given electrode disposition with N_c channels, and source space with N_d sources (dipoles) located on the cortical surface with fixed orientation perpendicular to it.

2.4.3. Proposed methodology for head model generation

In Figure **2-5** the pipeline of the head model generation stage is shown. It can be read as follows: (i) a volumetric segmentation of the different tissues are obtained from the MRI, (ii) a mesh of electrodes is coregistered and projected over the scalp surface, (iii) a volume conductor is established for the segmentation, (iv) a source space is selected, and finally (v) the Forward solution is done using the Finite Differences Reciprocity Method (FDRM).

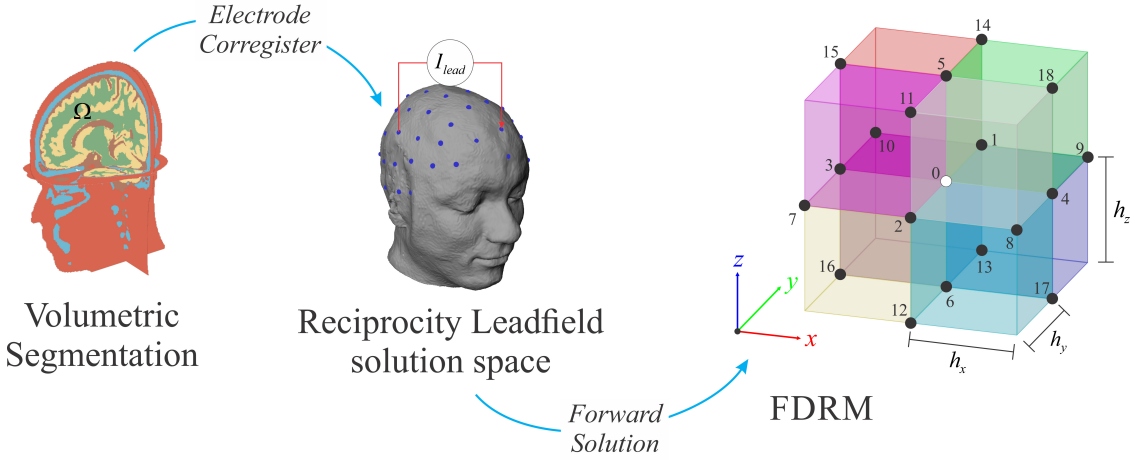

Figure 2-5: Forward modeling: The solution is carried out in a voxel-wise conductivity framework for a leadfield reciprocity space of a coregistered electrodes set. The solution of the forward problem is carried out using the FDRM algorithm.

Electrode co-registering
The forward model is strongly influenced by the correct electrodes positioning over the scalp

because the electrodes are directly related to the sources position and the described field propagation. In this work, we use affine transformations on the MRI to co-register predefined electrodes mesh in the head model and to wrap it over the scalp surface.

Source space

Forward modeling requires a source space located inside the brain. Due to most of the EEG signals are generated by sources located in the cerebral cortex, the dipole source space is restricted to the gray matter. To confine all sources of brain electrical activity to the gray matter, we apply a dilation-based morphological operator over the volumetric segmentation of white matter, resulting in a segmented middle area between the cortex and WM boundary. Thus, we initially triangulate a neocortex surface representation having more than 2×10^6 vertexes, which further are down-sampled using a quadratic edge decimation to produce approximately 10,000 vertexes. Every single vertex becomes a source position so that the triangulation procedure brings the connectivity map, containing the information about the spatial relationship between the neighbor sources to every single voxel. The schematic representation of the proposed methodology for producing the source space is presented in Figure **2-6**.

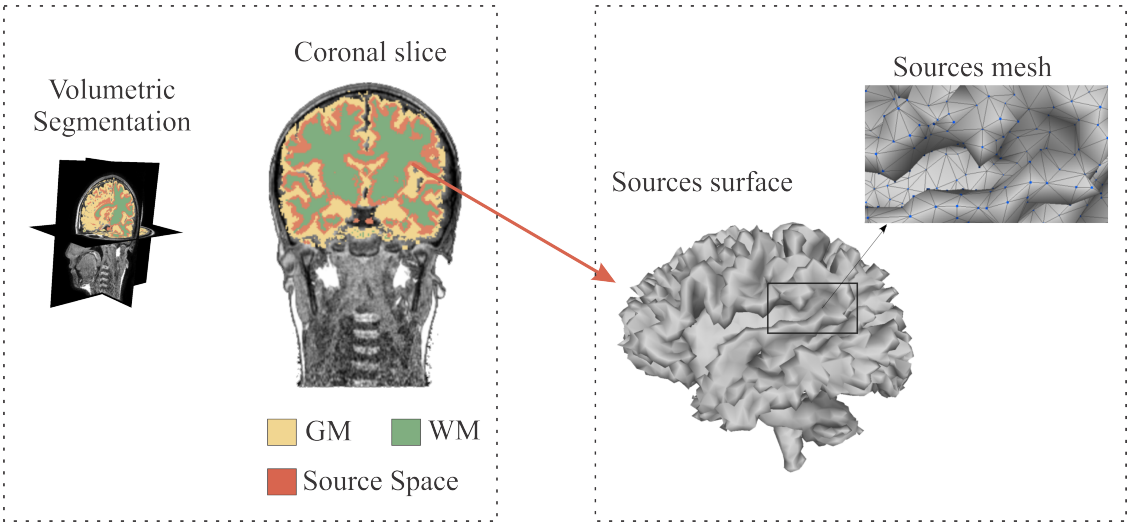

Figure 2-6: Source space dependent on MRI.

Conductivity values

For the different compartments the scalar conductivity values are fixed as display the Table **2-1**.

2.5. Bayesian Framework for ESI

The ESI goal is to obtain the neuronal activity as accurate as possible. It is done using the information provided by the EEG recordings and a defined head modeling [19]. Based

Tissue	$\sigma(S/m)$
Scalp	0.43
Skull	0.01
CSF	1.79
WM	0.14
GM	0.33

Table 2-1: Overview of the tissue conductivities. Values provided by [64].

on the forward model, EEG data can be generated assuming some active current dipoles. However, estimating the location and distribution of these current sources leads to an issue. Due to the relatively small number of electrodes measuring the brain electrical activity (a couple of hundred at best), and a large number of discretized brain activity generators (up to several thousand), it leads to a mathematical ill-posed problem. In short, the amount of information to be determined is much more than the available information. This problem is commonly referred to as the EEG inverse problem. Several techniques have been proposed to find a unique solution by minimizing the difference between the generated EEG data and the measured EEG data, i.e. the residuals. Each inverse technique will differ depending on the nature of the forward model and the optimized cost-function to find the optimal dipole parameters, i.e., the locations and the intensities of the dipoles. Mainly, distributed dipoles approaches are employed, which represent a highly under-determined but linear system. Classical and most popular distributed dipoles approach can be framed regarding a Weighted Minimum Norm criterion (WMN), which obtain a unique solution by optimizing an accuracy term and a regularization term in a carefully balanced way. Hence, we introduce a Bayesian statistical approach to solve the inverse problem for ESI. The Bayesian approach establishes the ESI as a linear problem formulated on a distributed source model, allowing to include multiple source priors for EEG source imaging. Additionally, a generalized cost function is derived, i.e. the free energy, that is optimized to find a unique solution using the Restricted Maximum Likelihood (ReML) algorithm. Finally, we show the Bayesian Framework for ESI, which can be used to compare different forward models depending on the measured EEG data.

2.5.1. Probability and Bayesian Inference

For the sake of simplicity, we will now drop notation depicting data from each EEG segment, and describe the inversion procedure for any segment of data $\boldsymbol{Y} \in \Re^{N_c \times N_t}$ with N_c number of channels and N_t time samples. Hence, $\boldsymbol{Y}$ is given by [19, 11]:

$$\boldsymbol{Y} = \boldsymbol{L}\boldsymbol{J} + \boldsymbol{\Xi}, \tag{2-3}$$

where $\boldsymbol{J} \in \Re^{N_d \times N_t}$ is the amplitude of the N_d current dipoles distributed through the cortical surface with fixed orientation perpendicular to it, and $\boldsymbol{L} \in \Re^{N_c \times N_d}$ is the lead field matrix linking the source amplitudes in $\boldsymbol{J}$ of the assumed dipoles on fixed locations to the electrical potential in EEG data $\boldsymbol{Y}$. We assume that the EEG measured data are affected by a zero mean Gaussian noise $\boldsymbol{\Xi} \in \Re^{N_c \times N_t}$ with covariance $\boldsymbol{Q}_{\Xi}$.
Generally, source estimation can be expressed by the expected value of the posterior source activity distribution, which can be computed from the input data using the Bayes' theorem, in the form:

$$p(\boldsymbol{J}|\boldsymbol{Y})=\frac{p(\boldsymbol{Y}|\boldsymbol{J})p(\boldsymbol{J})}{p(\boldsymbol{Y})}, \tag{2-4}$$

thereby, we can solve Equation (2-4) by assuming that $\boldsymbol{J}$ is a zero mean Gaussian process with prior covariance $cov(\boldsymbol{J}) = \boldsymbol{Q}$, with $\boldsymbol{Q} \in \Re^{N_d \times N_d}$. Thus, brain activity estimation, $\widehat{\boldsymbol{J}}$, is carried out by solving the widely known maximum-a-posteriori problem as follows:

$$\widehat{\boldsymbol{J}} = \underset{\boldsymbol{J}}{\operatorname{argmax}}\ p(\boldsymbol{J}|\boldsymbol{Y}) = \underset{\boldsymbol{J}}{\operatorname{argmax}}\ p(\boldsymbol{Y}|\boldsymbol{J})p(\boldsymbol{J}), \tag{2-5}$$

The optimization problem of Equation (2-5) yields the estimate $\widehat{\boldsymbol{J}}=\boldsymbol{Q}\boldsymbol{L}^T(\boldsymbol{Q}_{\Xi}+\boldsymbol{L}\boldsymbol{Q}\boldsymbol{L}^T)^{-1}\boldsymbol{Y}$, that requires prior knowledge about the sensor noise covariance $\boldsymbol{Q}_{\Xi}$ and the source covariance matrix $\boldsymbol{Q}$. In order to supply the sensor noise covariance, we set $\boldsymbol{Q}_{\Xi}=exp(\lambda_{\Xi})\boldsymbol{I}_{N_C}$ where $\boldsymbol{I}_{N_C} \in \Re^{N_C \times N_C}$ is an identity matrix scaled by a hyperparameter modulating the sensor noise variance λ_{Ξ} [50]. We use two different alternatives to supply the source covariance matrix $\boldsymbol{Q}$ where the sources are smoothed:

Multiple Sparse Priors (MSP): Where the source covariance matrix is constructed as a sum of a set of P patches $\{\boldsymbol{Q}_p, p{=}1,\ldots,P\}$ each one reflecting one potentially activated region of cortex, weighted by the respective hyperparameter λ_p, as follows [15]:

$$\boldsymbol{Q}=\sum_{p=1}^{P} \exp(\lambda_p)\boldsymbol{Q}_p, \tag{2-6}$$

Low-Resolution Tomography (LOR): Is assumed that the sources are smoothed, and multiple dipoles are related in focal region [47, 48]. A way to obtain a smoother is proposed in [21], where a Green's structural MRI is introduced, taking into account the inter-voxel distance and connections between sulci. The source covariance matrix, holding a Laplacian operator $\boldsymbol{\Delta} \in \Re^{D \times D}$, that aims to represent the groups of neurons with synchronized activation, seeking for smoothness:

$$\boldsymbol{Q} = \exp(\lambda_1)(\boldsymbol{L}^{\top}\boldsymbol{\Delta}^{\top}\boldsymbol{L}\boldsymbol{\Delta})^{-1}. \tag{2-7}$$

2.5.2. Free Energy as cost function

To estimate the hyperparameter set $\{\lambda_{\boldsymbol{\Xi}}, \lambda_{\boldsymbol{P}}\}$, we use the so termed free energy [65]. In this regard, for a given EEG recording and a certain forward model m, the free energy can be expressed as [39]:

$$F(m)=-\frac{N_t}{2}Tr(\boldsymbol{\Delta}^{-1}\boldsymbol{C})-\frac{N_t}{2}ln\,|\boldsymbol{\Delta}|-\frac{N_cN_t}{2}ln2\pi-\frac{1}{2}(\boldsymbol{\mu}-\boldsymbol{\eta})^T\boldsymbol{\Omega}^{-1}(\boldsymbol{\mu}-\boldsymbol{\eta})+\frac{1}{2}ln\left|\boldsymbol{\Upsilon}\boldsymbol{\Omega}^{-1}\right|, \quad (2\text{-}8)$$

where $\boldsymbol{\Delta} \in \Re^{N_c\times N_c}$ is the estimated model covariance, computed as $\boldsymbol{\Delta}=\boldsymbol{LQL}^\top+\boldsymbol{Q}_\Xi$; $\boldsymbol{C} \in \Re^{N_c\times N_c}$ is the measured data covariance, $\boldsymbol{\mu}, \boldsymbol{\eta} \in \Re^{N_p\times 1}$ are the prior and posteriors means of the hyperparameters $\{\lambda_\Xi, \lambda_p\}$. Likewise, $\boldsymbol{\Upsilon}, \boldsymbol{\Omega} \in \Re^{P\times P}$ are the posterior and prior hyperparameter covariances. $|\cdot|$ represent the matrix determinant operator.
Therefore, maximizing the free energy cost function estimated in (2-8) can be considered as a trade-off between the accuracy of the solution and the complexity of the solution. The accuracy (the first two terms) penalizes the difference in variance between the measured EEG data $\boldsymbol{Y}$ and the estimated solution $\widehat{\boldsymbol{Y}}=\boldsymbol{LJ}$. The complexity (the last two terms) gives a measure of the difficulty level to optimize the hyperparameters for a given prior. Hence, the free energy defined in Equation (2-8) can be divided as follows:

$$F(m)=accuracy(\lambda) - complexity(\lambda), \quad (2\text{-}9)$$

The Free Energy can be maximized using standard variational schemes [65]. To perform this optimization scheme, we use a greedy search (GS) algorithm. Further, the set of GS hyperparameters were tuned through the Restricted Maximum Likelihood (ReML) algorithm, as explained and detailed in [4, 15].

2.5.3. Bayesian model selection (BMS)

Now, suppose that we want to compare different forward models using the Bayesian Framework. So, making the dependency on a certain forward model m, Equation (2-4) is rewritten as [36]:

$$p(\boldsymbol{J}_m|\boldsymbol{Y},m)=\frac{p(\boldsymbol{Y}|\boldsymbol{J}_m,m)p(\boldsymbol{J}_m)}{p(\boldsymbol{Y}|m)}, \quad (2\text{-}10)$$

where $p(\boldsymbol{J}_m)$ represents the prior assumptions about the source activity and $p(\boldsymbol{Y}|m)$ the model evidence.
The log evidence after inversion $\log p(Y,\hat{\lambda})$, i.e. the free energy computed with the optimal set of estimated hyperparameters, provides an approximation to the log model evidence $\log p(\boldsymbol{Y}|m)$ [36, 35]. Thus, the free energy can be used for Bayesian model selection. Hence, some metrics based on the free energy values are defined to test the likelihood of obtaining a model in favor of another model, given the EEG data.

Fixed Effects analysis: The free energy values corresponding with different forward models m can be used to compare model performance in source reconstruction task, using Bayesian model selection [22]. In turn, free energy values can be evaluated in a fixed effects analysis comparing the log Bayes factors (ψ). For two models m_1 and m_2 the log Bayes factor is defined as:

$$\log(\psi_{(m_1,m_2)})=\frac{p(\boldsymbol{Y}|m_1)}{p(\boldsymbol{Y}|m_2)}=F(m_1)-F(m_2), \tag{2-11}$$

where $F(m_1)$ and $F(m_2)$ are the free energy corresponding with a model 1 and a model 2, respectively. The log group Bayes factor (Ψ) is defined as the sum of the individual log Bayes factors over N subjects as follows:

$$\log(\Psi)=\sum_{n=1}^{N}\log(\psi^n_{(m_i,m_j)}), \tag{2-12}$$

where, the subscripts i, j refer to the models being compared, and N is the number of subjects. According to [49], a model can be chosen in favor of another when there is a difference larger than three units. This criteria apply for both the log ψ and the log Ψ at group level. It is worth to note that Ψ is a simple index for direct model comparison and it does not account for group heterogeneity or outliers.

Random-effects analysis: The expected posterior model frequencies and exceedance probabilities quantify the probability that a particular model generated the data for any randomly selected subject, compared with the other models. In this sense, these metrics are calculated using a random-effects approach, treating each model as a random variable and estimating the parameters of a Dirichlet distribution that describes the probabilities for all considered models [57].

The expected posterior model frequency reflects the proportion of participants that support a certain model, and is defined as:

$$r_k=\frac{\alpha_k}{\alpha_1+...+\alpha_K}, \tag{2-13}$$

being k=1, ..., K and K the number of models, α_i with i=1, ..., K, the Dirichlet parameters and r_k representing the expected likelihood of obtaining the $k-th$ model over all the other models.

The exceedance probability represents the possibility that a model has the highest posterior probability, respect to other models, given the group data $\boldsymbol{Y}$:

$$\phi_k = p(r_k > r_j|\boldsymbol{Y};\boldsymbol{\alpha}), \tag{2-14}$$

where $j = 1, ..., K$ and $j \neq k$, $\boldsymbol{\alpha} = [\alpha_1, ..., \alpha_K]$ are the Dirichlet parameters. To quantify and establish the reliability obtained results based on the exceedance probabilities and the

expected posterior model frequency, the Bayesian omnibus risk (BOR) is commonly used [53]. It directly quantifies the probability that the expected posterior model frequencies are all equal to each other and therefore evaluates the probability that the observed findings may have occurred by chance. The BOR can be taken as an error rate, in that the rule establishes that when the BOR is smaller than 0.25, we can be confident in choosing the best model based on the results of the exceedance probabilities [53].

3 ESI performance when using individually-defined head models

3.1. Introduction

The goal of ESI is to obtain the neural generators of electrical brain activity measured on the scalp. It implies a direct influence between the forward model capabilities for closely describe the head structural patterns and the source imaging performance. To review this influence, we evaluate two approaches to enhance the model of brain structure in the EEG forward problem formulation: *i*) Incorporating progressively more realistic knowledge of the brain tissue morphology concerning each patient. *ii*) Varying the tissue model complexity by augmenting the number of segmented brain layers. In brief, this chapter is referred to the study of the forward model influence in the ESI task, mainly, the after-effects of including several tissues and personalized prior structural information.
Head models are built using the *Fieldtrip* Toolbox in the tissues segmentation, and the Finite Difference Reciprocity Method (FDRM) [9] as a numeric approximation to the forward solution. ESI and Bayesian Model Selection are made using the functions implemented in the Statistical Parametric Mapping software (SPM12) for neuroimaging.

3.2. Enhanced brain tissue modeling for improving the performance of ESI

With the aim of improving the performance of ESI, we evaluate two approaches to enhance the model of brain structure in the EEG forward problem formulation: *i*) Encouraging patient-dependent data by incorporating more realistic knowledge of the brain tissue morphology concerning each patient. For comparison, the anatomical structure priors are extracted from the following cases of image data: a standardized MRI template (NY), a demographic population atlas (AT), or a set of patient-specific MRI scans (PD). *ii*) Constructing a more precise volumetric tissue model by augmenting the number of segmented brain tissues. Namely, we contrast the following configurations of tissue model complexity: three-layer arrangement (noted as **3L**), including brain, skull, and scalp. **4L**, adding CSF to the **3L** configuration. **5L**, dividing the brain layer of **4L** in white matter and gray matter. The testing outline is shown in Figure **3-1**.

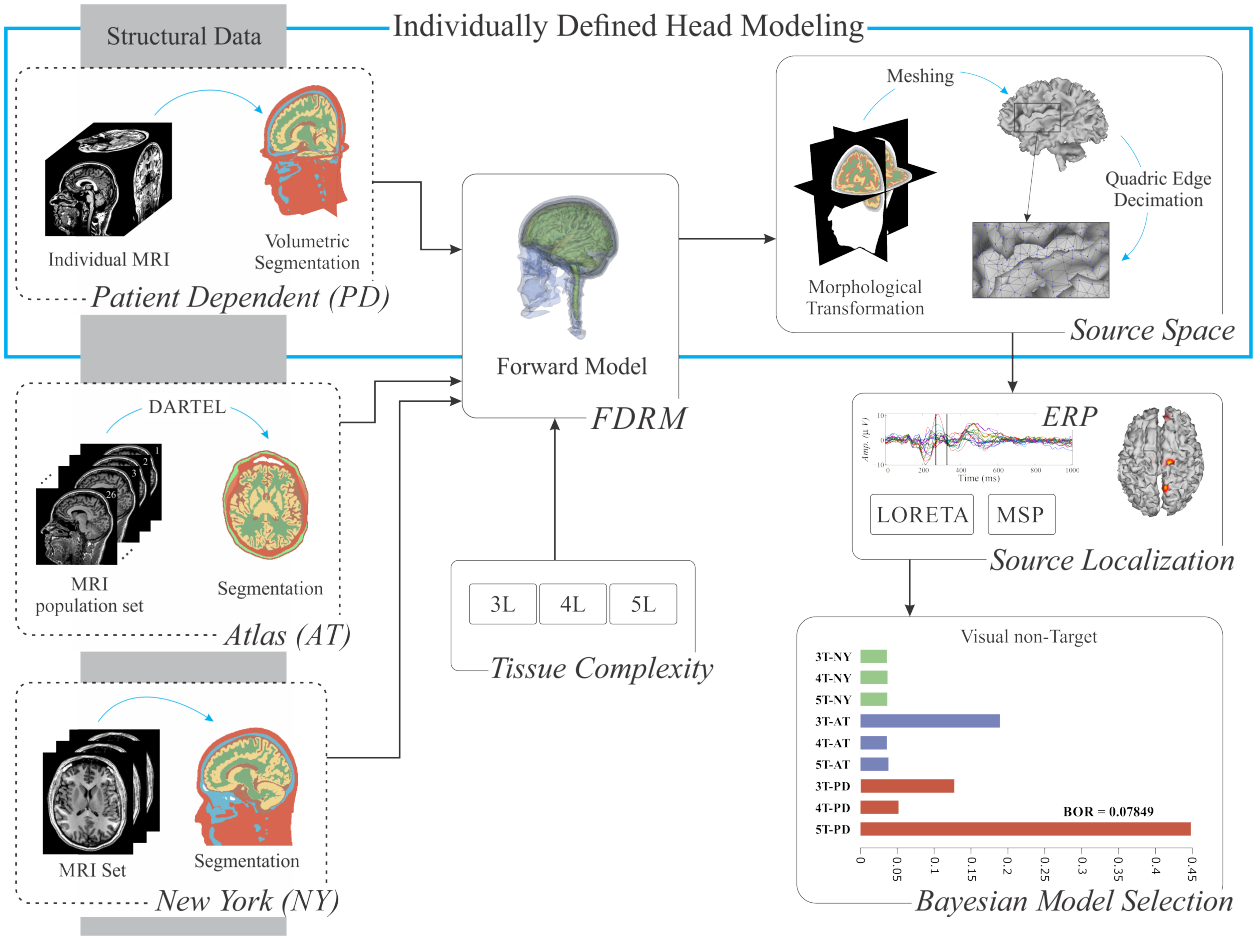

Figure 3-1: Schematic representation of the tested methodology to enhance the brain tissue model within the EEG forward problem formulation. The top row within the blue box shows the proposed individually defined head modeling, including patient dependent structural MRI, individual MRI segmentation, FDRM and individual source space modeling. Left middle and bottom boxes show the comparing structural information, namely, Atlas (AT) and New York (NY). The top middle panel shows the different tissue complexity (3L, 4L, and 5L). The remaining panel shows the source localization and the performance measure.

Evaluation of the proposed methodology to enhance the brain tissue model is accomplished within the Bayesian formulation of the EEG inverse problem as shown in Figure **3-1**, where the MSP and LOR methods are carried out as the ESI solution. Head models are constructed using the methodology described in chapter 2.

3.2.1. Participants and patient-dependent brain image measures

The brain image data were acquired from 25 children within an age range between 5 to 16 years old, having two socio-cultural levels (high–medium and low–medium). All patients were randomly selected from the preschool, elementary, and secondary courses at a few private and public schools of Manizales city. For legal purposes, the children's parents agreed to participate in the research through a written permission. According to the children's historical data, the exclusion criteria were established for mental retardation, individuals with neurological antecedents (history of head trauma, epilepsy, and related) or referring psychiatric disorders (psychiatric hospitalization history, autism, and similar).
From each child, two brain image datasets were acquired: an MRI collection supplying the anatomical priors of the brain tissues, and a *EEG/ERP* set that is employed for validation of the EEG source imaging performance.

MRI: A set of T1-MRI scans are acquired from the same 25 children under study, employing a 1,5 T General Electric OPTIMA MR 360 scanner with the following parameters: 1 mm $\times 1\, mm$ pixel size, T_R=6, T_E=1,8, T_I=450, and sagittal slices of 256×256 size and 1 mm spacing. For each child, three scans are performed to be further averaged (using the free surfer suite), yielding a single representative brain MRI with the goal of providing an enhanced signal–to–noise ratio.

EEG/ERP: The brain activity data were obtained following an oddball experimental paradigm for cognitive evoked potentials with rare visual stimuli, where each evoked stimulus lasted 130 ms, while the time delay between the onsets of two consecutive stimuli was 1 s. During each stimulation, the subjects had to pay attention to the rare stimulus (termed *target*) and count their occurrence, ignoring the presence of remaining stimuli (*non–targets*). The non–target stimuli were displayed on 80 % of the trials, whereas the target stimuli –on 20 % of remaining trials, resulting in approximately 160 non–target stimuli and 40 target stimuli. The EEG recordings were collected using 19 electrodes symmetrically placed at the standard positions of the international 10-20 system, operating a single *(Cadwell) Easy III EEG amplifier*. Data were subsampled at 250 Hz and segmented in 1-s epochs, which were averaged separately over each subject and stimulation condition. As a result, two ERPs were obtained following the different stimulus conditions for each subject, namely, visual target (**V-T**) and visual non-target (**V-nT**).

3.2.2. Head models integrating brain structure priors

For incorporating anatomical priors of the brain tissues in the EEG forward problem, we evaluate the ESI performance individually over the following head models:

Template-based head model (Noted as **NY**). A standardized volume conductor model that avoids any patient-dependent or population-dependent information. As a patterned template, we use the New York Head (NY) that is frequently used in neuroimage studies whenever an individual MRI is not available. NY allows segmentation of one symmetric head template (ICBM-152 v2009) into two tissue types (gray matter –GM, white matter –WM) and partition of another symmetric template (ICBM-152 v6) into non-brain tissues (CSF, skull, and scalp). Also, the segmentation of lower head part is extracted from an additional head template averaged over 25 subjects provided by [24]. Thus, the segmented head tissues together with extracted lower part are compounded into the NY head model.

Atlas head model (**AT**). An anatomical brain atlas is built to provide a more precise demographic tissue information about a concrete population sample. So, we built a generic atlas from the obtained 25 representative MRI scans, employing the Diffeomorphic Anatomical Registration (DARTEL) algorithm that generates a set of customized templates for the considered brain tissues [18]. The use of DARTEL non–linearly transforms all individual probabilistic partitions, initially provided by the *Statistical Parametric Mapping* (SPM) Matlab Toolbox, merging them into a single template. The registration procedure is conducted during a fixed number of iterations for increasing the template crispness. To construct from all patients the atlas that includes all tested tissues, DARTEL is applied using the following default parameters: Linear elastic energy regularization, Levenberg–Marquardt optimization, and six outer iterations.

Patient–dependent head model (**PD**). This model of prior information includes patient-dependent structure data individually and tends to provide a more specific knowledge of the geometry of each child's brain, performing an individual MRI segmentation of all considered brain tissues separately. Nevertheless, the resulting segmentation, which is accomplished using the FieldTrip pipeline [46], may contain some anatomic errors, like WM patches surrounded by skull or skull exposed outside scalp. Therefore, the segmentation is corrected to ensure that the GM tissue covers WM entirely, being contained by CSF at the same time. It is worth noting that the brain segmentation procedure includes the neck area extracted for each patient [31].

All considered head models are implemented using the methodology for the EEG forward solution proposed in [9]. Figure **3-2** displays some examples of the applied segmentation for the examined head models incorporating prior information.

3.2.3. Parameter selection

Source space. All sources of brain electrical activity are confined to the gray matter applying a dilation-based morphological operator over the volumetric segmentation of white

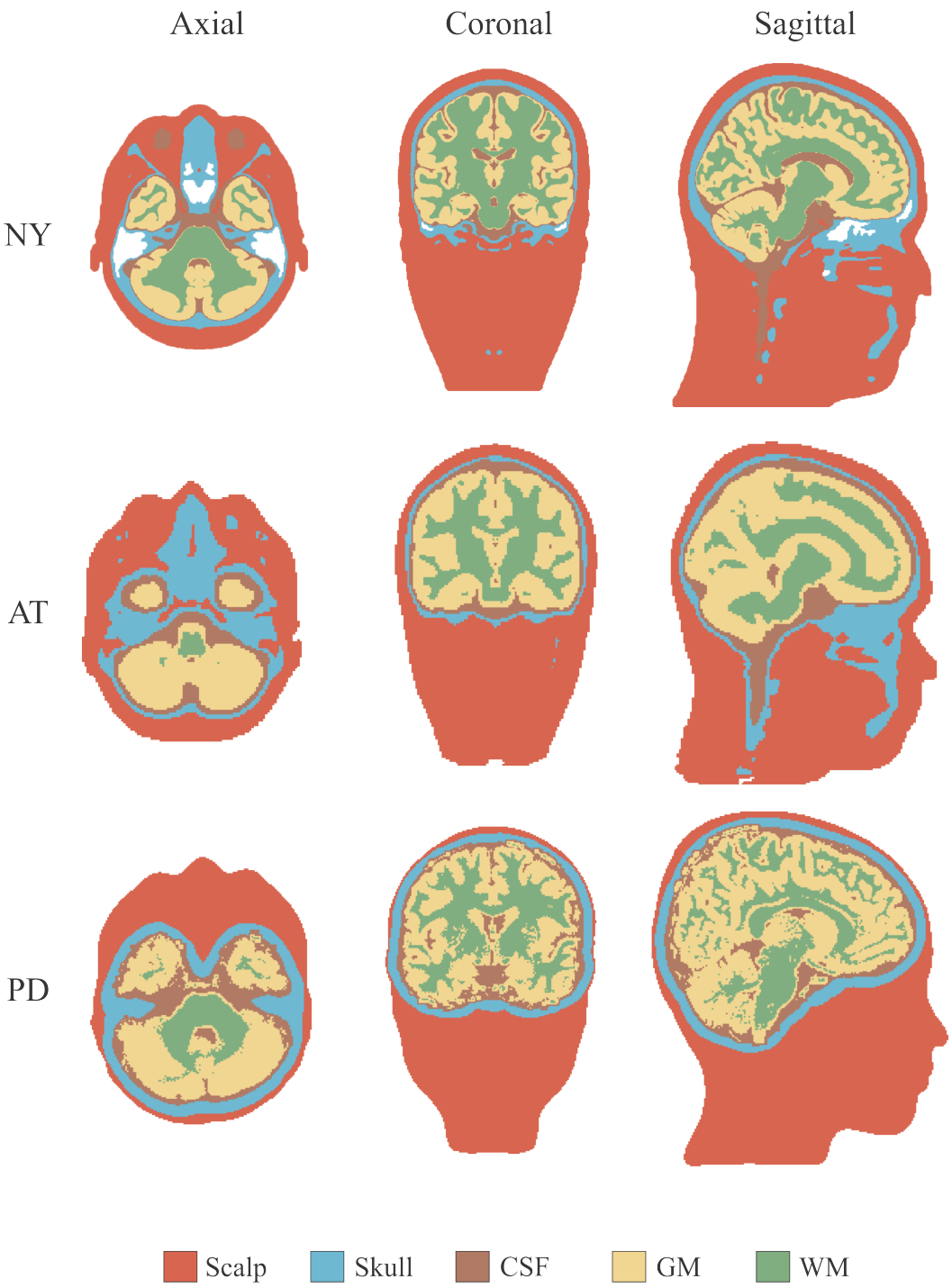

Figure 3-2: Exemplary of performed five–layered segmentation for the contrasted head models to incorporate prior information into the EEG forward model formulation.

matter, as shown in chapter 2. It results in a segmented middle area between the cortex and WM boundary, which is triangulated and downsampled using a quadratic edge decimation to produce approximately 10,000 vertexes.

Conductivity values. Based on the generated source space, then, the lead fields are calculated from the performed segmentation of brain tissues for the tested head model configuration (3L, 4L, and 5L), fixing the corresponding conductivity values to the suggested in table **2-1** [64].

3.2.4. Validating scenarios of ESI

In accordance with the evaluated approaches to enhance the brain tissue model, we explore the following nine scenarios for evaluating the direct EEG problem: **3L–NY**, **4L–NY**, **5L–NY**, **3L–AT**, **4L–AT**, **5L–AT**, **3L–PD**, **4L–PD**, and **5L–PD**.
In all scenarios, the source reconstruction of visual stimuli is validated using two ESI solutions: LOR and MSP. In the former case, the Laplacian operator $\mathbf{\Delta}$ is included to represent groups of neurons with synchronized activation (see Equation 2-7), modeling spatial coherence. In the case of MSP, the priors, needed to compute the set of covariance components, are constructed as a sum of patches, each one reflecting one potentially activated region of cortex weighted by the respective hyperparameter (see Equation 2-6). For either ESI solution, priors are implemented by the Statistical Parametric Mapping (SPM12) software package, where the number of covariance components is fixed to 1024 for MSP, which are formed by sampling from evenly spaced columns of the coherence matrix as to cover the cortical surface entirely. Besides, the MSP hyperparameters are tuned by maximizing the Free energy through the Restricted Maximum Likelihood approach under a greedy search algorithm.
During validation, we employ Bayesian Model Selection (BMS), making the same group studies as in [52]. This approach is based on the free energy as an approximation to the Bayesian log evidence, yielding a reliable measure that shows which model is more probable to generate the available data [58]. To this end, we compare the Free energy values of the inverse solutions over subjects, corresponding with the ERPs elicited by each stimulation condition. Then, the log group Bayes factor ($\rho_L \in \Re$), the expected likelihood ($\rho_K \in \Re^+$) and the Bayesian omnibus risk – BOR ($\rho_B \in \Re^+$) are computed. In the log group Bayes factor, one model can be chosen in favor of the other when there is a difference larger than three points. Additionally, the exceedance probability expresses the belief that a model has the highest posterior probability regarding the other ones. Besides, the BOR quantifies the likelihood that the expected posterior model frequencies are all equal. Thus, if the BOR is smaller than 0,25, the best model selected according to the exceedance probability is trustworthy.

3.2.5. Results

Performed source imaging using anatomic structure priors

With the purpose of a better data visualization, all values of log Bayes factor (ψ) are represented through the radar charts that display the source imaging performance data in a radial

pattern as shown in Figure **3-3**. The star chart holds the ψ computed for the worst testing scenario of each patient in reference to the other ones. As a result, the worst scenario fall to zero, and the other are shown in positive differences. Therefore, the higher this computed factor, the better the model performs the EEG source reconstruction [49]. Note that each colored string depicts the performance obtained by a single subject, where the gray circle is drawn for the cases of significant Bayes factor, having differences that are greater than three points.

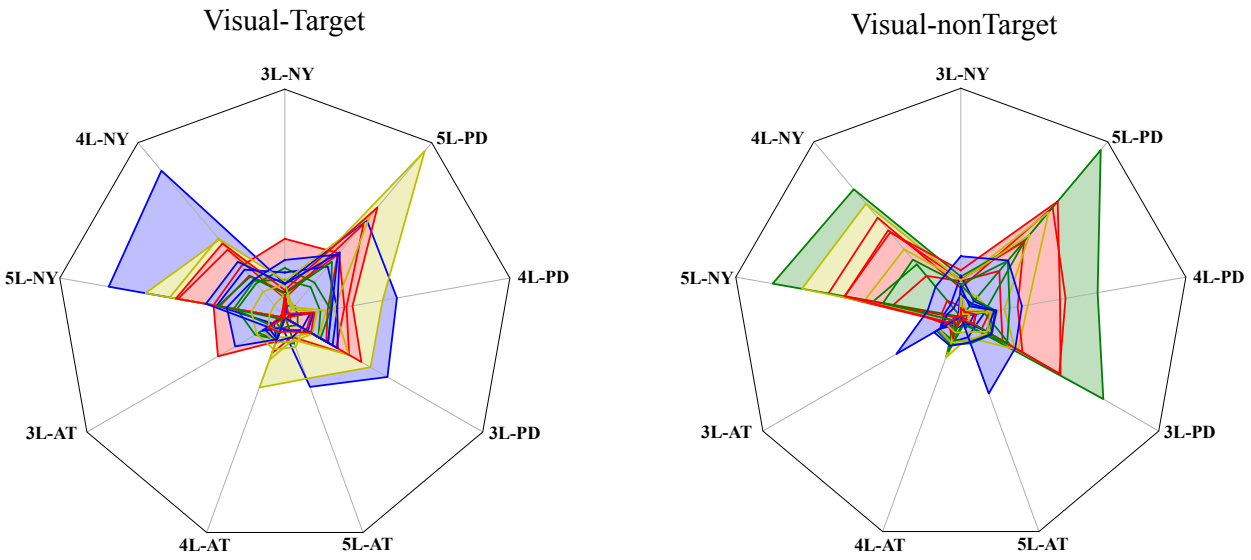

(a) LOR

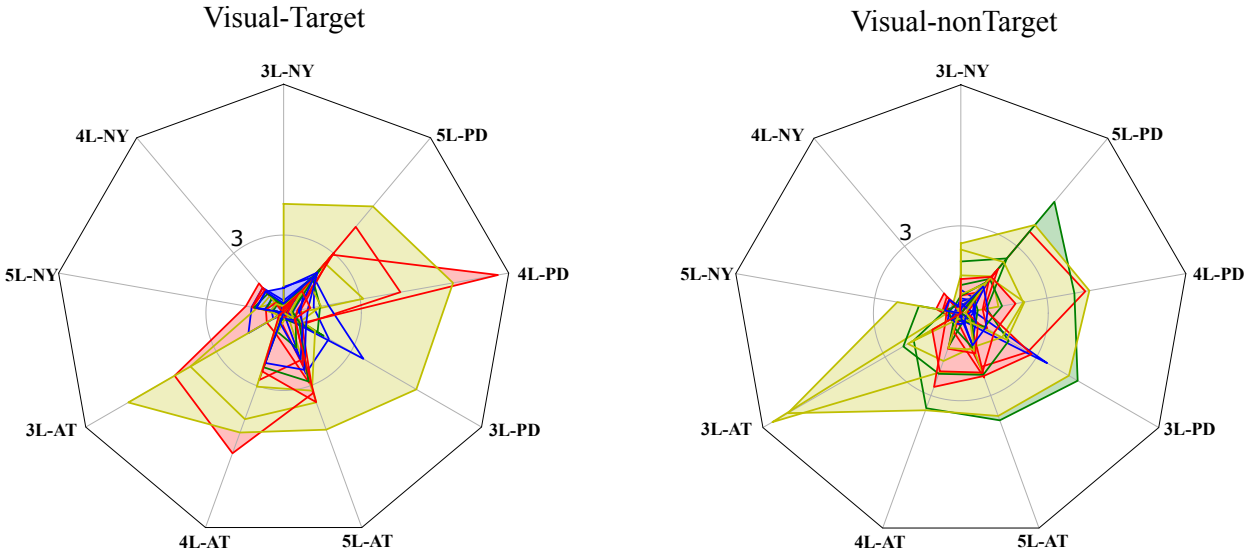

(b) MSP

Figure 3-3: Radar chart showing the ψ values achieved by LOR as ESI solutions for each scenario and patient

Figure 3.3(a) displays the achieved performance by LOR source imaging solution, showing that the testing scenarios of NY produce the highest values of ψ regardless of the considered stimuli condition. At the same time, the AT head models perform the worst. In the case of MSP solution, Figure 3.3(b) shows that all testing scenarios of NY models produce the lowest values of ψ regardless of the considered stimuli. Concerning the AT models, the radar charts also show that the reconstruction accuracy improves, meaning that the inclusion of structural priors using the study population enhances the tissue model. However, the highest values of ψ are achieved by the PD head models, resulting in the best model for incorporating information about head tissues in the EEG forward problem. Another aspect to consider is the variability provided by each ESI solution for every patient. Thus, although MSP produces much fewer outliers than the LOR solution does, it is hard to select the best scenario during validation of the individually–defined forward modeling.

Bayesian model selection of EEG source imaging methods

The BMS for group studies is employed, aiming to generalize the performance results achieved by the examined ESI solutions across the whole patient set. Thus, BMS identifies the best source reconstruction through a random effect analysis, assuming that each subject is drawn from a large population of subjects so that his response represents an independent sample from the overall distribution [7]. We conduct BMS through the expected posterior probability and Bayesian omnibus risk (BOR), comparing the log model evidence for each reconstruction at the group level.

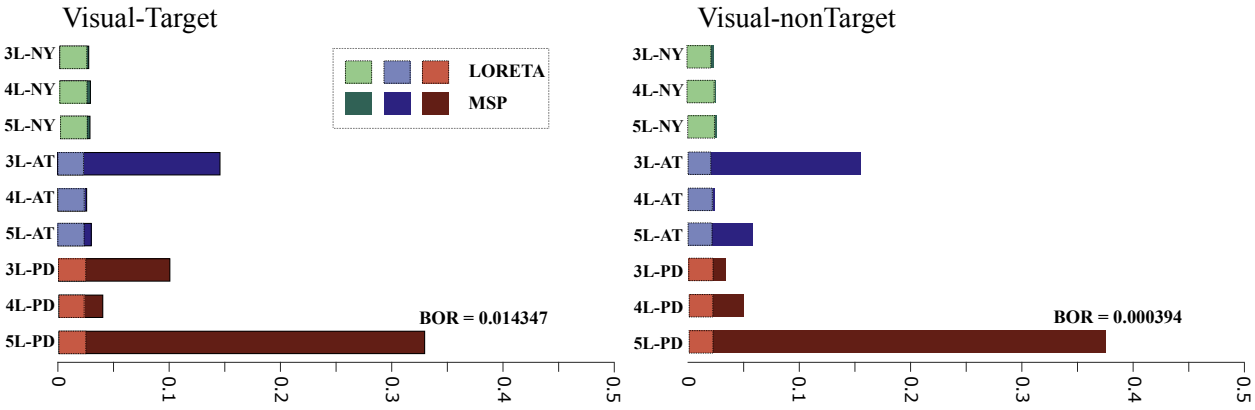

Figure 3-4: Results of Bayesian model selection shown as the expected posterior probability and Bayesian omnibus risk assessed by each testing scenario of brain tissue model. Here, both LOR and MSP are used as ESI solution methods.

Figure **3-4** presents the performed results, comparing together all the testing scenarios of MSP and LOR solutions. It is worth noting that the confidence for the expected posterior probability is adequate for the considered visual stimuli (BOR lesser than 0,25).

On the other hand, MSP performs better results than LOR in all stimuli condition despite the tested scenario of head model, making evident the superiority of the former solution regarding the achieved reconstruction accuracy. This effect may be explained relaying the fact that the LOR solution tends to fail in detecting deep sources. Furthermore, the deeper the actual source, the more blurred is the current density estimated by LOR [48]. On the contrary, the MSP algorithm embraces the entire cortical surface (both focal and deep), identifying the patches that better reproduce the neural source distribution, and thus, enabling a more accurate reconstruction of the superficial and deep sources [15].

Figure **3-5** displays the considered ESI solutions performed for a randomly selected patient, allowing to explain the above-described effect of different accuracy on the deep reconstructed sources. Besides, the NY head models are implemented due to the simplicity of their incorporated priors, having the lowest influence on the source reconstruction. The obtained source reconstruction reveals that LOR spreads the activity over the entire cortical mesh although the identified prevailing areas tend to be less scattered as the number of modeled tissues increases. On the contrary, MSP focuses the most on the visual-processing related areas (like the visual cortex in the posterior brain area), becoming more evident as the number of tissues increases. Consequently, due to the showed outstanding superiority, we further consider the MSP solution in the following procedures.

Comparison of brain tissue models

For the MSP source imaging, we compare the enhancing scenarios of brain tissue model through the explained log model evidence at the group level.

Figure **3-6** shows that the best brain structure is **5L-PD** that certainly achieves the highest expected posterior probability (the top bar highlighted with red) with high confidence since the BOR value is much lower than 0,25. The second highest performance is achieved by the **3L-AT** testing scenario, outperforming even the **3L** and **4L** layer arrangements of the PD models. Further, there is no apparent benefit in selecting one of the remaining scenarios of PD or AT models. In fact, except in the case of **5L** configuration, either model behaves similarly. Nonetheless, all scenarios tested for the **NY**-based brain tissue models plainly reach the lowest probability of a model generating the observed data, confirming that this is the worst strategy of incorporating anatomical priors.

Regarding the used tissue model complexity, the performed Bayesian model selection only infers that the five-layer arrangement provides the most substantial source reconstruction performance. Other patterns of complexity tissues are comparable regardless of the used stimuli and combined head model to integrate the brain structure priors.

To inspect the quality of the ESI solution, we provide a visual inspection of the obtained source reconstruction for a representative subject, using the best-achieved head model for each tested scenario, i.e., **5L-PD**, **3L-AT**, and **5L-NY**.

Thus, Figure **3-7** shows the sensor space data, namely, an example of ERP and scalp topo-

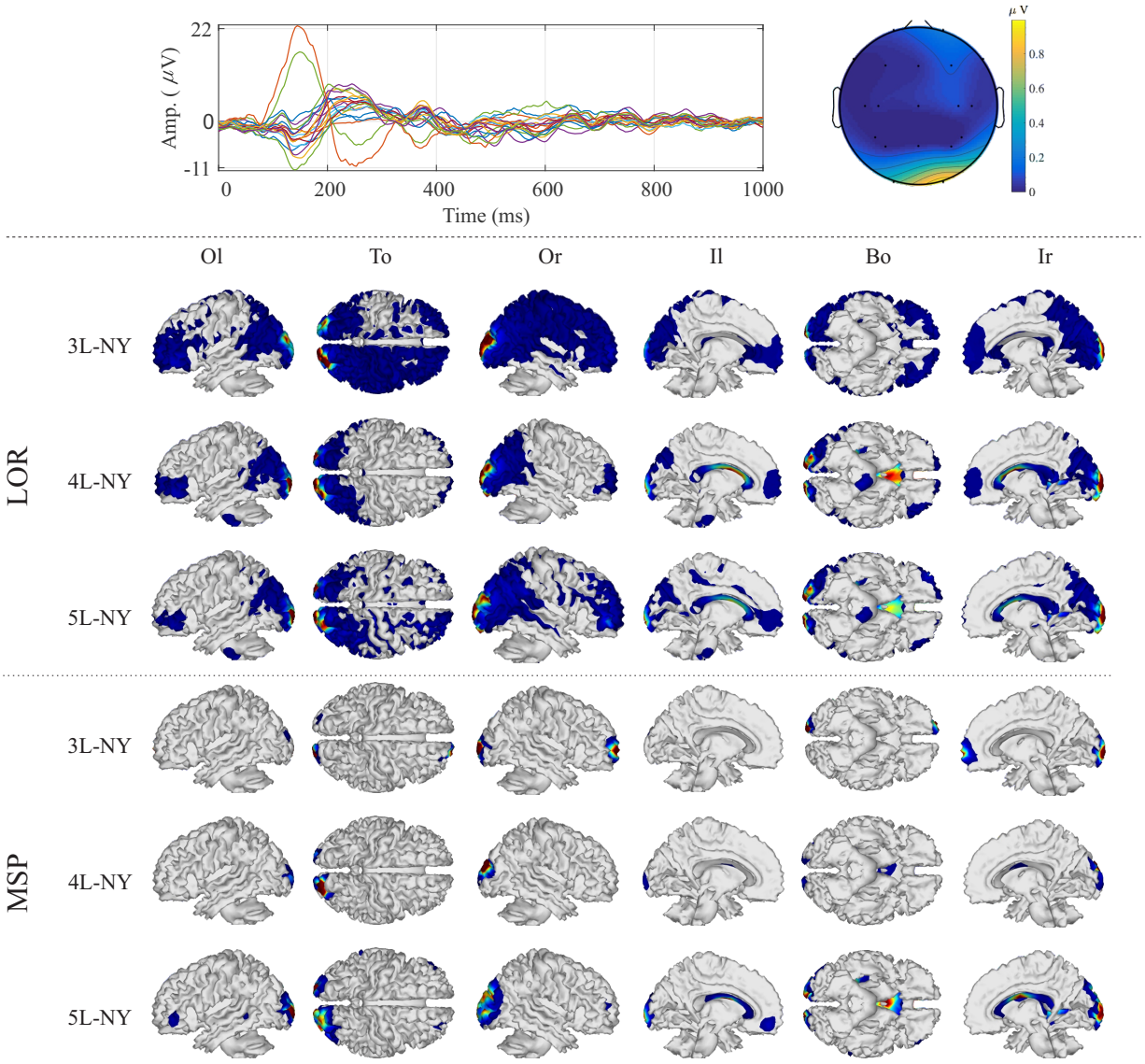

Figure 3-5: Achieved source reconstructions with NY models for both ESI methods. Top: Sensor space - ERP and topographic map. Bottom: Reconstructed activity. Views: Outside right (Or), Outside left (Ol), Top (To), Bottom (Bo), Inside right (Ir) and Inside left (Il).

graphy, as well as the results of the source reconstruction (dipole-wise power). Both, scalp topography and source activity, are averaged in the time range from 100 to 200 *ms* (typically, termed N200 component), which contains brain-specific responses related to the processing of visual stimuli [14]. The ERP waveform shows a prominent temporo-occipital negative peak around 180 *ms*, which is mostly associated with visual processing.

Moreover, the reconstructed activity localizes some components in the vicinity of the temporal lobe, covering the visual cortices for all the tested models. However, **5L-NY** model

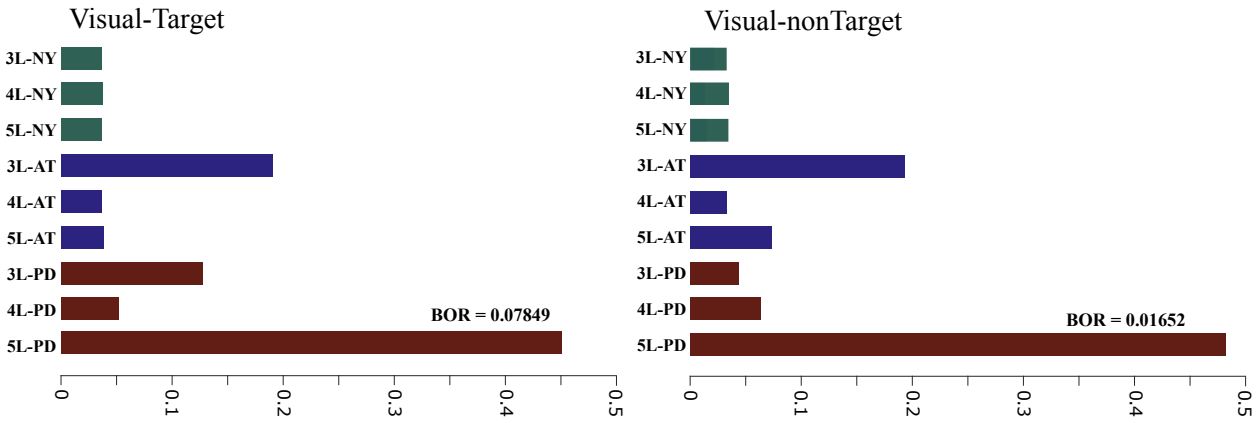

Figure 3-6: Results of Bayesian model selection shown as the expected posterior probability and Bayesian omnibus risk assessed by each testing scenario of brain tissue model. Here, MSP is used as ESI solution method.

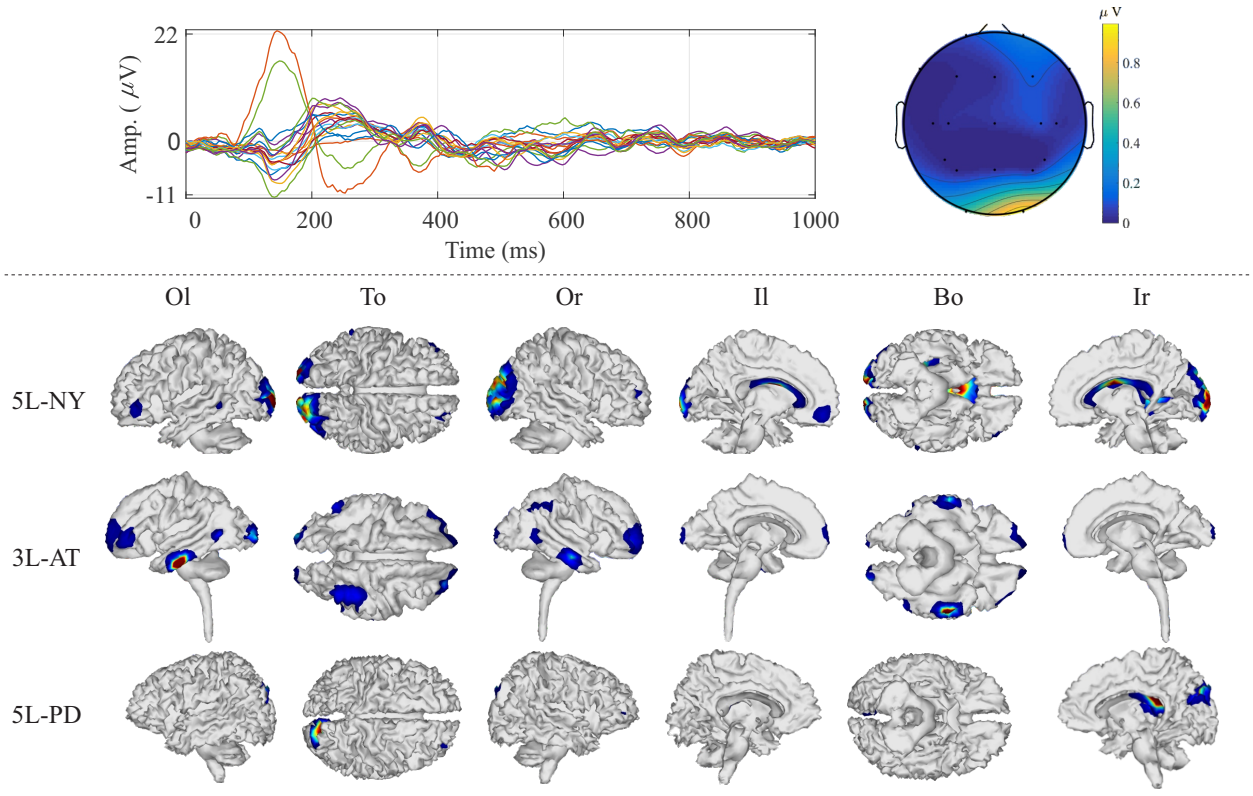

Figure 3-7: ESI solution for a representative subject using the best-achieved head models for each structural prior information, namely, **5L-PD**, **3L-AT**, and **5L-NY**. Top: Sensor space - ERP and topographic map. Bottom: Reconstructed activity. Views: Outside right (Or), Outside left (Ol), Top (To), Bottom (Bo), Inside right (Ir) and Inside left (Il).

spreads the brain activity, which makes that some activations appear in non-visual related areas. **3L-AT** activates the middle temporal gyrus, that has some visual-related task. Additionally, in **5L-PD**, an activity patch seems over the posterior cingulate gyrus, which occurs when a high demand of visual processing/discrimination is required, confirming that this kind of priors enhances the reconstruction of neural activity.
Another aspect to consider is the accuracy of brain activity source localization achieved by the volumetric brain segmentation that we model through the number of tissues incorporated into the head model. From the results performed by MSP, Figure **3-8** shows that including CSF segmentation (i.e., **4L)** overperforms the conventionally used 3-layer head model just in the case of **NY** tissue morphology. Otherwise, the discrepancy in performance between both configurations may vary from case to case.

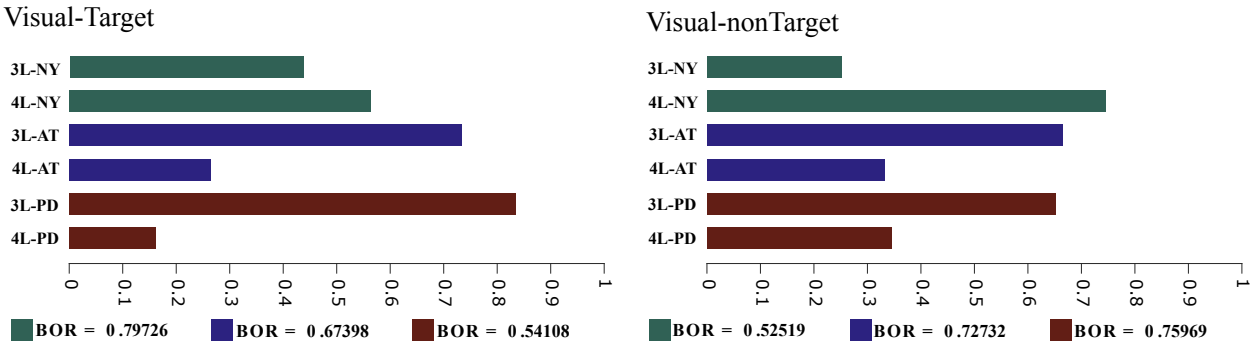

Figure 3-8: Results of Bayesian model selection shown as the expected posterior probability and Bayesian omnibus risk, comparing, within each structural prior information, the 3L and 4L head models. Here, MSP is used as ESI solution method.

Also, we investigate the distinction between the white and gray matter in the volumetric brain segmentation, proving that the highest model complexity (5L) performs almost the best for each method to include the anatomical priors and regardless the elicited stimulus (see Figure **3-6**).

3.3. Discussion

With the aim of enhancing the ESI performance regarding the anatomical structure priors used to feed the forward modeling, we propose two approaches for improving the model of brain structures: i) Including anatomical patient/population dependent data. ii) Enhancing the complexity of the head model by augmenting the number of considered brain tissues. Through the above-validated results on real EEG/ERP data, the following findings are worth mentioning:

Contribution of anatomical structure priors. For incorporating anatomical priors of the brain tissues in the EEG forward problem, the radar charts show that the Patient–dependent

head model is the best-considered head model that is followed by the AT models, and being NY the worst representation. This result agrees with the commonly reported criterium of modeling structure priors, stating that the more the individual anatomical information, the smaller the source localization error [22]. However, modeling of the brain tissues is very sensitive to wrong shape approximations of the target population (form, size, and demographics), which lead to significant errors of source localization [13]. Thus, the widely used NY head model is not aware of any demographic details, and consequently, is very likely to be far more representative of any particular target population. For reducing the shape differences between modeled and actual head tissues, the AT model builds an averaged atlas extracted from a population as similar as possible to the target. Another aspect to consider is the variability observed between the examined patient group as shown by the radar charts in Figure **3-3**. Hence, some in-congruent approximations may appear, making the brain structure deteriorate by the head segmentation complexity (see Figure **3-4**). It should be noticed that, in practice, additional factors decrease the ESI performance. Most representative sources of error include measurement and physiological noise of the EEG, incorrect electrodes placement and insufficient contact with the scalp, and errors derived from the ill-posed inverse problem. As a result, the patient-specific head model that provides the inclusion of more realistic knowledge of the brain tissue morphology allows increasing the most the performance of EEG source localization.

Impact of volumetric brain segmentation. One of the main aspects of head modeling is the number of considered tissues. Here, we investigate two modifications to the classical 3-layered approximation of the head: The inclusion of a CSF compartment, and the distinction between white and gray matter in the brain.

In the last years, it has been established that the 3-layers head model is a strong simplification of the reality. Therefore, several improvements of this model have been suggested, being the inclusion of a CSF compartment, the most common one [66, 58, 64]. However, we obtain that the discrepancy in performance between neglecting CSF or adding this tissue to the conventionally used configuration may vary from case to case. The drop in performance may be explained because of some small changes in CSF layer thickness can provide a significant effect on EEG signal magnitudes in several standard visual paradigms[51].

Moreover, we divide the brain into the white and gray matter. This distinction has not been considered in most of the previous studies on source analysis. Instead, the separation between the white and gray matter makes the volumetric segmentation perform almost the best for each method to include the anatomical priors, demonstrating that neglecting this tissue division diminishes notably the ESI solution results [1]. Therefore, the volumetric brain segmentation influences heavily on the forward and inverse problems, so, it must be carried out as accurately as possible. As in the previous case, when using atlas head models, this distinction does not improve the ESI performance. It might be produced because of discrepancies between the modeled and the real subject's anatomy. Therefore, one might

conclude that a more accurate model in brain size and shape is better than a not so detailed model of WM and GM tissues. However, when using patient-dependent data, results are once again, significantly improved. As a result, we observe that the more realistic the head modeling, i.e., patient dependent MRI and a more significant number of layers, the better the source reconstruction.

Source space. A more realistic modeling of the sulci and gyrus of the brain enhances the individually-defined forward model. In practice, canonical source reconstruction is employed that pools anatomical data from multiple subjects, being very susceptible to inter-subject variability in cortical anatomy that poses a factor of an inaccurate tissue modeling [40]. To cope with this issue, we propose a cortical mesh that is transformed anatomically to produce the subject-specific mesh. For this, we confine all sources of brain electrical activity within the gray matter by applying a dilation-based morphological operator over the volumetric segmentation of white matter, resulting in a segmented middle area between the cortex and WM boundary. As an additional advantage, our source space generation proposal is efficiently adaptable to a wide class of prior structural information as it does not require any manual intervention for ensuring that sources are enclosed within the gray matter. As a concrete example Figure **3-7** shows some focalized sources in the posterior cingulate gyrus, which in fact must be related to the tested visual stimulus [33]. Therefore, even that the patient-dependent approaches demand the cortical surface extraction from an individual's MRI, an efficient method for computing the EEG forward problem, along with the head model, is essential to provide a more accurate localization of very focal sources.

Forward Model solver. In the literature, several forward modeling methodologies have been employed, being BEM the most used one. However, BEM solves the forward potentials only for the interfaces between two neighbor tissues. As a result, BEM interpolates the potential in the scalp induced by a dipole inside the GM. Additionally, BEM works mainly with three layers, namely scalp, skull, and brain. Consequently, to consider more versatile forward models, we use a volumetric technique named FDRM, which allows: i) including more complex tissues at a negligible computational effort, and ii) adapting to the voxelized structural information of a patient using his segmentation of the MRI data.

The benefit of individually-defined source reconstruction. As regards the influence of the used dipole source localization, we also compare two well-established approaches: LOR and MSP. The former ESI approach reconstructs mostly surface sources, favoring the simplest head model (i.e., NY template) that produces the lesser detailed description of the tissue structures. Instead, the MSP method enables the reconstruction of superficial as well as deep sources, embracing the entire cortical surface. Additionally, MSP takes advantage of the measured EEG data to select the neural activity reconstruction model (sparse or distributed), using to a greater extent the prior information provided by the PD head models and the

EEG. As a result, a more elaborate ESI solution also enhances the individually-defined source reconstruction.

The last aspect to consider is the lack of a ground truth when using real data. Thus, although one solution might appear more focal than another, there is not a reason why it should be more accurate. Consequently, the model evidence provided by the Bayesian ESI solution is a plausible tool for comparing the ESI performance when using several head models, as has been previously demonstrated in [22, 15, 58]. Consequently, it is worth noticing that we are claiming that the best model is the more probable depending on the data.

4 Final Remarks

4.1. General Conclusions and Main Contributions

Methodology for generating personalized forward models
We propose a methodology for generating personalized forward models, allowing the inclusion of prior structural information and different levels of model complexity. The proposed methodology takes into account priors of anatomical structure extracted from the following cases of image data: a standardized MRI template (NY), a demographic population atlas (AT), or a set of patient-specific MRI scans (PD). Additionally, different configurations of tissue model complexity are selectable: three-layer arrangement (**3L**), including brain, skull, and scalp. **4L**, adding CSF to the **3L** configuration. **5L**, dividing the brain layer of **4L** in white matter and gray matter. As a result, our proposed methodology is suitable for generating head models with different levels of prior information.

Methodology for estimating a patient-dependent source space
We develop a methodology for estimating source space using the structural information provided by the patient-specific MRI. In our approach, we applied 3D morphological transformations to the white matter to obtain a cortical mesh that properly describes the free-form sulci disposition of the gray matter. Our method guarantees that the vertexes of the estimated mesh are fully contained in the GM area. Additionally, the quadric edge collapsing method allows the reduction of the vertexes (source positions), maintaining the sulci forms in the GM.

Evaluation of performance of forward models in the ESI task
We present an evaluation and comparison study of the forward models in the EEG source reconstruction task. Group studies are performed using the Bayesian Model Selection (BMS) framework, allowing to infer the most probable head model to generate the EEG data, within a set of possible models. This framework support all the comparisons made in this dissertation. Obtained results show that the source reconstruction is strongly influenced by the model complexity and the prior anatomic information.

4.2. Future work

Enhancing the model of tissue conductivity
Previous studies have reported that some electrical conductivities of brain tissue are highly anisotropic [38, 25], which generate topography errors when they are not considered. However, the head model is commonly approximated as a volume conductor with isotropic conductivity. In this dissertation, the white matter and the skull were simplified using isotropic conductivity values. So, future work could include the anisotropic conductivities in WM and skull to investigate its effect on ESI task.

Increasing the model complexity
In this work, we evaluate how the variation of the tissue model complexity by augmenting the number of segmented brain layers influences the ESI task. Hence, we fit a set of testing scenarios in which the model complexity was increased including several brain tissues (Scalp, Skull, CSF, GM, WM). Briefly, results show that the more complex the head model, the better the ESI solution. However, many other tissues and essential properties as the anisotropy can be included in future works due to the flexibility of the FDRM methodology.

Generalizing the findings
In the present context, the inferences are based on the approximated model evidence given by the free energy, which takes into account the data fit and the model complexity. Nevertheless, group studies may be carried out using another metric that considers other relevant criteria, such as reproducibility of results across datasets and the predictive validation of results. In this sense, it is worth to note that all of the above findings are obtained for a specific dataset. So, future work could show whether the present results can be extrapolated to other datasets.

Bibliography

[1] Acar, Zeynep A. ; Makeig, Scott: Effects of forward model errors on EEG source localization. In: *Brain topography* 26 (2013), Nr. 3, p. 378–396

[2] Allen, Nicola J. ; Barres, Ben A.: Neuroscience: glia-more than just brain glue. In: *Nature* 457 (2009), Nr. 7230, p. 675–677

[3] Baillet, Sylvain ; Mosher, John C. ; Leahy, Richard M.: Electromagnetic brain mapping. In: *IEEE Signal processing magazine* 18 (2001), Nr. 6, p. 14–30

[4] Belardinelli, Paolo ; Ortiz, Erick [u. a.]: Source reconstruction accuracy of MEG and EEG Bayesian inversion approaches. In: *PloS one* 7 (2012), Nr. 12, p. e51985

[5] Berger, Hans: Über das elektrenkephalogramm des menschen. In: *European Archives of Psychiatry and Clinical Neuroscience* 87 (1929), Nr. 1, p. 527–570

[6] Britton, J ; Jervis, BW ; Grünewald, RA: Extracting single trial event related potentials. In: *IEE Proceedings-Science, Measurement and Technology* 147 (2000), Nr. 6, p. 382–388

[7] Chen, Jingyuan E. ; Glover, Gary H.: Functional magnetic resonance imaging methods. In: *Neuropsychology review* 25 (2015), Nr. 3, p. 289–313

[8] Chernecky, Cynthia C. ; Berger, Barbara J.: *Laboratory tests and diagnostic procedures*. Elsevier Health Sciences, 2007

[9] Cuartas-Morales, E. ; Acosta-Medina, C.D. [u. a.]: iLU Preconditioning of the Anisotropic-Finite-Difference Based Solution for the EEG Forward Problem. (2015), Jun, p. 408–418

[10] Cuffin, B N.: EEG localization accuracy improvements using realistically shaped head models. In: *IEEE Transactions on Biomedical Engineering* 43 (1996), Nr. 3, p. 299–303

[11] Dale, Anders M. ; Sereno, Martin I.: Improved localizadon of cortical activity by combining EEG and MEG with MRI cortical surface reconstruction: a linear approach. In: *Journal of cognitive neuroscience* 5 (1993), Nr. 2, p. 162–176

[12] Doetsch, Fiona: The glial identity of neural stem cells. In: *Nature neuroscience* 6 (2003), Nr. 11, p. 1127

[13] von Ellenrieder, Nicolás ; Muravchik, Carlos H. ; Nehorai, Arye: Effects of geometric head model perturbations on the EEG forward and inverse problems. In: *IEEE Transactions on Biomedical Engineering* 53 (2006), Nr. 3, p. 421–429

[14] Folstein, Jonathan R. ; Van Petten, Cyma: Influence of cognitive control and mismatch on the N2 component of the ERP: a review. In: *Psychophysiology* 45 (2008), Nr. 1, p. 152–170

[15] Friston, Karl ; Harrison, Lee ; Daunizeau, Jean ; Kiebel, Stefan ; Phillips, Christophe ; Trujillo-Barreto, Nelson ; Henson, Richard ; Flandin, Guillaume ; Mattout, Jérémie: Multiple sparse priors for the M/EEG inverse problem. In: *NeuroImage* 39 (2008), Nr. 3, p. 1104–1120

[16] Fuchs, Manfred ; Drenckhahn, Ralf ; Wischmann, H ; Wagner, Michael: An improved boundary element method for realistic volume-conductor modeling. In: *IEEE Transactions on Biomedical Engineering* 45 (1998), Nr. 8, p. 980–997

[17] Garey, Laurence J.: *Brodmann's 'localisation in the cerebral cortex'*. World Scientific, 1994

[18] Goto, Masami ; Abe, Osamu ; Aoki, Shigeki ; Hayashi, Naoto ; Miyati, Tosiaki ; Takao, Hidemasa ; Iwatsubo, Takeshi ; Yamashita, Fumio ; Matsuda, Hiroshi ; Mori, Harushi [u. a.]: Diffeomorphic Anatomical Registration Through Exponentiated Lie Algebra provides reduced effect of scanner for cortex volumetry with atlas-based method in healthy subjects. In: *Neuroradiology* 55 (2013), Nr. 7, p. 869–875

[19] Grech, Roberta ; Cassar, Tracey ; Muscat, Joseph ; Camilleri, Kenneth P. ; Fabri, Simon G. ; Zervakis, Michalis ; Xanthopoulos, Petros ; Sakkalis, Vangelis ; Vanrumste, Bart: Review on solving the inverse problem in EEG source analysis. In: *Journal of neuroengineering and rehabilitation* 5 (2008), Nr. 1, p. 25

[20] Hallez, Hans ; Vanrumste, Bart [u. a.]. *Dipole estimation errors in EEG source localization due to not incorporating anisotropic conductivities of white matter in realistic head models*. Oktober 2007

[21] Harrison, Lee M. ; Penny, W ; Ashburner, J ; Trujillo-Barreto, N ; Friston, KJ: Diffusion-based spatial priors for imaging. In: *NeuroImage* 38 (2007), Nr. 4, p. 677–695

[22] Henson, R N. ; Mattout, J [u. a.]: Selecting forward models for MEG source-reconstruction using model-evidence. In: *NeuroImage* 46 (2009), Mai, Nr. 1, p. 168–76. – ISSN 1095–9572

[23] Herculano-Houzel, Suzana: The human brain in numbers: a linearly scaled-up primate brain. In: *Frontiers in human neuroscience* 3 (2009)

[24] Huang, Yu ; Parra, Lucas C. [u. a.]: The New York Head- a precise standardized volume conductor model for EEG source localization and tES targeting. In: *NeuroImage* 140 (2016), p. 150–162

[25] Huiskamp, Geertjan ; Vroeijenstijn, Maurice ; van Dijk, René ; Wieneke, George ; van Huffelen, Alexander C.: The need for correct realistic geometry in the inverse EEG problem. In: *IEEE Transactions on Biomedical Engineering* 46 (1999), Nr. 11, p. 1281–1287

[26] Jaskowski, Piotr ; Verleger, Rolf: Amplitudes and latencies of single-trial ERP's estimated by a maximum-likelihood method. In: *IEEE Transactions on biomedical engineering* 46 (1999), Nr. 8, p. 987–993

[27] Jatoi, Munsif A. ; Kamel, Nidal ; Malik, Aamir S. ; Faye, Ibrahima ; Begum, Tahamina: A survey of methods used for source localization using EEG signals. In: *Biomedical Signal Processing and Control* 11 (2014), p. 42–52

[28] Johnson, IP: Morphological peculiarities of the neuron. In: *Brain Damage and Repair*. Springer, 2004, p. 33–45

[29] Kandel, Eric R. ; Schwartz, James H. ; Jessell, Thomas M. ; Siegelbaum, Steven A. ; Hudspeth, A J. [u. a.]: *Principles of neural science*. Vol. 4. McGraw-hill New York, 2000

[30] Kilic, S ; Gencer, NG ; Baykal, Buyunnan: Comparison of methods for extracting of evoked potentials. In: *Engineering in Medicine and Biology Society, 2003. Proceedings of the 25th Annual International Conference of the IEEE* Vol. 3 IEEE, 2003, p. 2495–2498

[31] Lanfer, B ; Scherg, M ; Dannhauer, Moritz ; Knösche, Thomas R. ; Burger, Martin ; Wolters, Carsten H.: Influences of skull segmentation inaccuracies on EEG source analysis. In: *NeuroImage* 62 (2012), Nr. 1, p. 418–431

[32] Lange, Daniel H. ; Pratt, Hillel ; Inbar, Gideon F.: Modeling and estimation of single evoked brain potential components. In: *IEEE transactions on BioMedical Engineering* 44 (1997), Nr. 9, p. 791–799

[33] Leech, Robert ; Sharp, David J.: The role of the posterior cingulate cortex in cognition and disease. In: *Brain* 137 (2013), Nr. 1, p. 12–32

[34] Liu, Mingyu ; Ji, Hongbing ; Zhao, Chunhong: Event Related Potentials Extraction from EEG Using Artificial Neural Network. In: *Image and Signal Processing, 2008. CISP'08. Congress on* Vol. 1 IEEE, 2008, p. 213–215

[35] López, JD ; Litvak, Vladimir ; Espinosa, JJ ; Friston, K ; Barnes, Gareth R.: Algorithmic procedures for Bayesian MEG/EEG source reconstruction in SPM. In: *NeuroImage* 84 (2014), p. 476–487

[36] López, JD ; Penny, William D. ; Espinosa, JJ ; Barnes, Gareth R.: A general Bayesian treatment for MEG source reconstruction incorporating lead field uncertainty. In: *NeuroImage* 60 (2012), Nr. 2, p. 1194–1204

[37] Luck, Steven J.: *An introduction to the event-related potential technique*. MIT press, 2014

[38] Marin, Gildas ; Guerin, Christophe ; Baillet, Sylvain ; Garnero, Line ; Meunier, Gérard: Influence of skull anisotropy for the forward and inverse problem in EEG: simulation studies using FEM on realistic head models. In: *Human brain mapping* 6 (1998), Nr. 4, p. 250–269

[39] Martínez-Vargas, Juan D. ; López, Jose D. ; Baker, Adam ; Castellanos-Dominguez, German ; Woolrich, Mark W. ; Barnes, Gareth: Non-linear parameter estimates from non-stationary MEG data. In: *Frontiers in Neuroscience* 10 (2016)

[40] Mattout, Jérémie ; Henson, Richard N. ; Friston, Karl J.: Canonical source reconstruction for MEG. In: *Computational Intelligence and Neuroscience* 2007 (2007)

[41] Michel, Christoph M. ; Murray, Micah M. ; Lantz, Göran ; Gonzalez, Sara ; Spinelli, Laurent ; de Peralta, Rolando G.: EEG source imaging. In: *Clinical neurophysiology* 115 (2004), Nr. 10, p. 2195–2222

[42] Munck, de J. ; Peters, Maria J.: A fast method to compute the potential in the multisphere model. In: *IEEE transactions on biomedical engineering* 40 (1993), Nr. 11, p. 1166–1174

[43] Niedermeyer, Ernst ; da Silva, FH L.: *Electroencephalography: basic principles, clinical applications, and related fields*. Lippincott Williams & Wilkins, 2005

[44] Nishiyama, Akiko ; Yang, Zhongshu ; Butt, Arthur: Astrocytes and NG2-glia: what's in a name? In: *Journal of anatomy* 207 (2005), Nr. 6, p. 687–693

[45] Noctor, Stephen C. ; Martínez-Cerdeño, Verónica ; Kriegstein, Arnold R.: Contribution of intermediate progenitor cells to cortical histogenesis. In: *Archives of neurology* 64 (2007), Nr. 5, p. 639–642

[46] Oostenveld, Robert ; Fries, Pascal ; Maris, Eric ; Schoffelen, Jan-Mathijs: FieldTrip: open source software for advanced analysis of MEG, EEG, and invasive electrophysiological data. In: *Computational intelligence and neuroscience* 2011 (2011), p. 1

[47] Pascual-Marqui, Roberto D. ; Michel, Christoph M. ; Lehmann, Dietrich: Low resolution electromagnetic tomography: a new method for localizing electrical activity in the brain. In: *International Journal of psychophysiology* 18 (1994), Nr. 1, p. 49–65

[48] Pascual-Marqui, Roberto D.: Review of methods for solving the EEG inverse problem. In: *International journal of bioelectromagnetism* 1 (1999), Nr. 1, p. 75–86

[49] Penny, Will D. ; Stephan, Klaas E. [u. a.]: Comparing dynamic causal models. In: *Neuroimage* 22 (2004), Nr. 3, p. 1157–1172

[50] Phillips, Christophe ; Rugg, Michael D. ; Friston, Karl J.: Systematic regularization of linear inverse solutions of the EEG source localization problem. In: *NeuroImage* 17 (2002), Nr. 1, p. 287–301

[51] Rice, Justin K. ; Rorden, Christopher ; Little, Jessica S. ; Parra, Lucas C.: Subject position affects EEG magnitudes. In: *NeuroImage* 64 (2013), p. 476–484

[52] Rigoux, Lionel ; Stephan, Klaas E. ; Friston, Karl J. ; Daunizeau, Jean: Bayesian model selection for group studies – revisited. In: *Neuroimage* 84 (2014), p. 971–985

[53] Rigoux, Lionel ; Stephan, Klaas E. ; Friston, Karl J. ; Daunizeau, Jean: Bayesian model selection for group studies - revisited. In: *Neuroimage* 84 (2014), p. 971–985

[54] Sabbatini, Renato: Neurons and synapses: The history of its discovery. In: *Brain & mind magazine* 17 (2003), p. 39–40

[55] Saleheen, H I. ; Ng, K T.: A new three-dimensional finite-difference bidomain formulation for inhomogeneous anisotropic cardiac tissues. In: *IEEE transactions on biomedical engineering* 45 (1998), Januar, Nr. 1, p. 15–25. – ISSN 0018–9294

[56] Shirvany, Yazdan ; Porras, Antonio R. ; Kowkabzadeh, Koushyar ; Mahmood, Qaiser ; Lui, Hoi-Shun ; Persson, Mikael: Investigation of brain tissue segmentation error and its effect on EEG source localization. In: *Engineering in Medicine and Biology Society (EMBC), 2012 Annual International Conference of the IEEE* IEEE, 2012, p. 1522–1525

[57] Stephan, Klaas E. ; Penny, Will D. ; Daunizeau, Jean ; Moran, Rosalyn J. ; Friston, Karl J.: Bayesian model selection for group studies. In: *Neuroimage* 46 (2009), Nr. 4, p. 1004–1017

[58] Strobbe, Gregor ; van Mierlo, Pieter [u. a.]: Bayesian model selection of template forward models for EEG source reconstruction. In: *NeuroImage* 93 (2014), p. 11–22

[59] Tatum IV, William O.: *Handbook of EEG interpretation*. Demos Medical Publishing, 2014

[60] Toga, Arthur W. ; Mazziotta, John C.: *Brain mapping: the methods.* Academic press, 2002

[61] Turovets, Sergei I. ; Poolman, Pieter ; Salman, Adnan ; Malony, Allen D. ; Tucker, Don M.: Conductivity Analysis for High-Resolution EEG. In: *2008 International Conference on BioMedical Engineering and Informatics* c (2008), Mai, p. 386–393. ISBN 978–0–7695–3118–2

[62] Ullian, Erik M. ; Sapperstein, Stephanie K. ; Christopherson, Karen S. ; Barres, Ben A.: Control of synapse number by glia. In: *Science* 291 (2001), Nr. 5504, p. 657–661

[63] Valdés-Hernández, Pedro A. ; Von Ellenrieder, Nicolás [u. a.]: Approximate average head models for EEG source imaging. In: *Journal of neuroscience methods* 185 (2009), Nr. 1, p. 125–132

[64] Vorwerk, Johannes ; Cho, Jae-Hyun [u. a.]: A guideline for head volume conductor modeling in EEG and MEG. In: *NeuroImage* 100 (2014), p. 590–607

[65] Wipf, David P. ; Owen, Julia P. [u. a.]: Robust Bayesian estimation of the location, orientation, and time course of multiple correlated neural sources using MEG. In: *NeuroImage* 49 (2010), Nr. 1, p. 641–655

[66] Wolters, C H. ; Anwander, A [u. a.]: Influence of tissue conductivity anisotropy on EEG / MEG field and return current computation in a realistic head model : A simulation and visualization study using high-resolution finite element modeling. In: *NeuroImage* 30 (2006), p. 813 – 826